

Validation of Nonlinear Finite Element Analysis on Reinforced Concrete Slab under Concentrated Out-of-plane Load Combined with Uniaxial In-plane Load Based on Case Study

Master thesis

for the degree of Master of Science in Structural Engineering,

Delft University of Technology



By

Yanxin Zhou

26th November 2018

Validation of Nonlinear Finite Element Analysis on Reinforced Concrete Slab under Concentrated Out-of-plane Load Combined with Uniaxial In-plane Load Based on Case Study

By

Yanxin Zhou

in partial fulfilment of the requirements for the degree of

Master of Science

in Structural Engineering, Concrete structures
at the Delft University of Technology,

Thesis committee: Prof.dr.ir. D.A. Hordijk

Dr.ir. M.A.N. Hendriks

Dr.ir. E.O.L. Lantsoght

26th November 2018

Acknowledgement

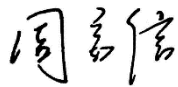
Firstly, I would like to express my appreciation to Dr.ir. M.A.N. Hendriks, my great supervisor who introduced me this interesting topic and guided me all through the process, for giving me valuable suggestions not only in academic aspects but also the way to become an engineer.

Then, I would like to thank Dr.ir. E.O.L. Lantsoght, who gave me great help, for showing me the rigorous attitude that one should have when doing research. This motivated me to overcome the obstacles patiently. I would also thank Prof.dr.ir. D.A. Hordijk. Your valuable suggestions guided me when I lost my direction.

In addition, I would like to thank my friends, for sharing all the happiness and sadness with me in these years. This experience is unforgettable and meaningful in my life.

Finally, the greatest appreciation to my parents, for your understanding and selfless support. Because of you, I could have the opportunity to experience more and try to be myself.

谢谢我的父母。是你们的理解和无私支持，让我体验到意义非凡的两年。



Delft,

26th November 2018

Abstract

Finite element analysis is becoming a popular tool for engineers recently. Nonlinear finite element analysis is more advanced due to that it can deal with the nonlinearity of structures, which leads to more accurate approximation of structural behaviour. In Model Code 2010, nonlinear finite element analysis, which belongs to the higher level of approximation, can predict the structural behaviour with refined physical parameters but by devoting more time to the analysis. This leads to better accuracy. Thus, it is important to study how to apply nonlinear finite element analysis to approximate the structural strength.

When it comes to the existing design codes, the shear design methods of reinforced concrete slabs loaded in uniaxial in-plane force are developed from the tests of beams rather than slabs, which may lead to the underestimation of the design resistance. Through experiments of seven slabs, a related study of the validity of existing shear design methods has been performed by Bui *et al.* (2017). However, there is no existing literature about the application of nonlinear finite element analysis towards the reinforcement concrete slabs mentioned above so far. In this thesis, one single nonlinear finite element analysis is applied to seven slabs of experiment to study the validation of nonlinear finite element analysis on the RC slabs without shear reinforcement loaded in concentrated out-of-plane load and uniaxial in-plane loads. The validation is studied by comparing results from finite element analysis, experiment and finite element analysis from Nana *et al.* (2017), which mainly includes shear load – displacement curve, development of crack pattern, failure modes and the influence of uniaxial load on the structural behaviour. In addition, the shear capacity under uniaxial in-plane load is studied by comparing results from analytical assessment based on existing codes, experiment and nonlinear finite element analysis.

When compared with experiment, nonlinear finite element analysis shows a close shear capacity of all seven slabs but stiffer structural behaviour. The development of cracks is similar to the observation of experiment. The failure modes indicated by nonlinear finite element analysis is more likely punching shear rather than one-way shear that is demonstrated in the experiment. The influence of increasing uniaxial compression on shear capacity is larger than what is observed in experiment while increasing tension has smaller influence. By comparing the prediction of shear capacity from experiment, existing codes and nonlinear finite element analysis, it can be concluded that NLFEA is unconservative in prediction of shear capacity of the RC slabs without shear reinforcement loaded in concentrated out-of-plane loads and uniaxial in-plane loads. Some suggestions are given for further study. Improvement of modelling is suggested. For instance, finer mesh could lead to more accurate results, and insights of bond-slip reinforcement could generate more precise results. Furthermore, the study of safety formats is suggested in further study to consider the uncertainty due to random variation of material properties. In addition, more experiments and nonlinear finite element analysis are suggested to get insights of the influence of uniaxial loads on structural behaviour of RC slabs without shear reinforcement.

Content

1.	Introduction	1
1.1	Background and problems	1
1.2	Methods and objectives.....	2
2.	Assessment methods	3
2.1	Analytical assessment of shear capacity of reinforced concrete slabs under uniaxial loads in existing codes.....	3
2.2	Numerical assessment method	6
2.3	Multi-level assessment method.....	9
3.	Case study of slab without in-plane load	14
3.1	Experiment by Bui <i>et al.</i> (2017).....	14
3.2	Nonlinear finite element model on S2 by Nana <i>et al.</i> (2017)	19
3.3	Modelling assumptions.....	23
3.4	Modelling choices	25
3.5	Alternative modelling.....	31
3.6	Results of modelling.....	34
3.7	Results of alternative modelling	40
3.8	Discussion of results.....	41
4.	Case study of slabs with uniaxial in-plane load	45
4.1	Experiment by Bui <i>et al.</i> (2017).....	45
4.2	Modelling of the uniaxial in-plane loading system	50
4.3	Results of modelling.....	52
4.4	Discussion of results.....	55
5.	Conclusion.....	59
5.1	Conclusion of slab without uniaxial in-plane load	59
5.2	Conclusion of slabs with uniaxial in-plane load	59
5.3	Suggestions for further study	60
	Reference	62
	Annex – calculation of shear capacity according to EC2 and ACI 318-14	64

1. Introduction

This master thesis is mainly about the nonlinear finite element analysis applied to the reinforced concrete slabs without shear reinforcement loaded in uniaxial tension or compression. In this chapter, research and progression about the shear capacity study of reinforced concrete (RC) slabs loaded in concentrated load in gravity direction are reviewed. The existing problems are stated as well. Based on the study of RC slabs, the interest and topic of this master thesis is proposed. The methods and objectives of this master thesis are demonstrated as well.

1.1 Background and problems

Reinforced concrete slabs are common in modern civil engineering constructions. For example, RC slabs can be used in multi-level buildings and concrete bridges. In practice, loading condition applied on RC slabs could be complex. The failure modes of RC slabs loaded with a concentrated load can be in three ways, bending, one-way shear and punching shear. The bending failure is the desired failure mode because bending allows structures to have ductile deformation and redistribution of internal force before collapse (Shu 2017). Shear failure is undesired because it is brittle. The collapse of structure happens suddenly. Thus, a lot of researches focus on the shear behaviour of RC slabs. In the complex loading condition, RC slabs can be loaded in uniaxial in-plane force, which is caused by the imposed deformation, wind, earthquake etc. This uniaxial in-plane force has influence on the shear behaviour of RC slabs. The research on this influence and the validation of assessment methods is important.

There are four assessment methods to be applied to the study of shear capacity of RC slabs, namely experiments, field tests, analytical assessment and numerical assessment. In terms of experiment, Shu (2017) reviewed and summarized the experiment of three failure modes of RC slabs respectively. It can be concluded that there is rarely experiments about the study of the influence of uniaxial in-plane load on the shear resistance of reinforced concrete slabs. Noticing that under the shear load, reinforced concrete structures may be simultaneously subjected to the axial tensile or compressive forces, and that the shear design rules for slabs are mostly derived from shear tests on beams and may lead to an underestimation of the shear resistance of one-way slabs (Lantsoght *et al.*, 2013), Bui *et al.* (2017) designed a set of experiment to verify the shear design codes on slab tests with uniaxial load and to study the influence of uniaxial loads on shear capacity of RC slabs without shear reinforcement.

For RC slabs, assessment methods are usually applied to the same case in recent research to see the validation of each method. For example, three series of research (a: Lantsoght *et al.* (2013) & Belletti *et al.* (2014); b: Shu (2017); c: Bui *et al.* (2017) & Nana *et al.* (2017)) studied the validation of assessment methods by applying them on the same case. In Model Code 2010, analytical and numerical assessment are integrated and called the concept of Levels-of-Approximation (LoA). In Shu (2017), this is called Multi-level Assessment Strategy. Within this method, higher the level is, more accurate results can be obtained and more time and skill is needed. Thus, 3D nonlinear finite element analysis with continuum elements with full-bonded reinforcement and higher with bond-slip reinforcement are the two most accurate approximation methods.

Finite element method is representative for numerical simulation. When it comes to the design of RC slabs, finite element method is inevitable. Finite element method can deal with the model that has complex geometry and material properties. Linear and nonlinear analysis methods are included in finite element method. Nonlinear analysis usually produces more accurate results because it considers the nonlinear properties of the structure and materials. Nonlinear finite element analysis (NLFEA) has become a popular and valid method to simulate the structural behaviour. The Dutch Guideline (Hendriks *et al.*, 2017) gives a set of suggestions to safely apply NLFEA, including the modelling of structures, analysis choices, verification in terms of limit state and the presentation of results. However, based on the literature review, there is no application of nonlinear finite element analysis to the RC slabs under concentrated out-of-plane load and uniaxial in-plane load. Thus, this master thesis will study the application of NLFEA to the RC slabs under concentrated out-of-plane load and uniaxial in-plane load tested by Bui *et al.* (2017).

1.2 Methods and objectives

In this master thesis, a single nonlinear finite element analysis will be applied to model the experiment by Bui *et al.* (2017) to investigate the validation of NLFEA on the RC slabs without shear reinforcement under uniaxial loads. The existing assessment methods are reviewed, which includes the provision of analytical assessment (Eurocode 2 and ACI 318-14), numerical assessment and multi-level assessment. In addition, the experiment by Bui *et al.* (2017) and the NLFEA on one of the slab by Nana *et al.* (2017) is introduced as the case study. Then, nonlinear finite element analysis with continuum elements is demonstrated. By comparing the results from NLFEA and experiment, some alternative NLFEA are applied to improve the modelling. Analytical assessment according to EC2 and ACI 318-14 is performed and stated in Annex. In this thesis, the study of slab without uniaxial in-plane load is described first, then is the study of slabs with uniaxial in-plane load. Based on the results from experiment, existing codes and NLFEA, the discussion and conclusion are made.

The objective of this thesis is the validation of nonlinear finite element analysis on the RC slabs without shear reinforcement loaded in concentrated out-of-plane load and uniaxial in-plane loads. First, the proper modelling of slabs is performed including several iterations and improvements. Second, comparison of results from finite element analysis, experiment and finite element analysis from Nana *et al.* (2017) is made, which mainly includes shear load – displacement curve, development of crack pattern, failure modes and the influence of uniaxial load on the structural behaviour. In addition, the shear capacity under uniaxial in-plane load is studied by comparing results from analytical assessment based on existing codes, experiment and nonlinear finite element analysis. Finally, the validation of NLFEA on the RC slabs without shear reinforcement loaded in concentrated out-of-plane load and uniaxial in-plane loads is discussed and concluded. Some suggestions are delivered for further study.

2. Assessment methods

2.1 Analytical assessment of shear capacity of reinforced concrete slabs under uniaxial loads in existing codes

2.1.1 Eurocode 2

According to EN 1992-1-1 chapter 6.2.2, Members not requiring design shear reinforcement, the design shear resistance is given as:

$$V_{Rd,c} = \left[C_{Rd,c} k (100 \rho_l f_{ck})^{1/3} + k_1 \sigma_{cp} \right] b_w d$$

With the minimum design shear resistance:

$$V_{Rd,c} = (v_{\min} + k_1 \sigma_{cp}) b_w d$$

Where:

$$k = 1 + \sqrt{\frac{200}{d}} \leq 2$$

f_{ck} is the characteristic compressive strength of concrete, no larger than 90 Mpa

$C_{Rd,c}$ is the empirical factor for characteristic shear capacity

ρ_l is reinforcement ratio of longitudinal reinforcement, $\rho_l = \frac{A_{sl}}{b_w d} < 0.02$

A_{sl} is the area of tensile reinforcement

b_w is the smallest width of the cross-section in the tensile area

d is the effective depth of the cross section

σ_{cp} is the stress due to axial force applying on the concrete cross section

The values of $C_{Rd,c}$, k_1 and v_{\min} can be found in National Annex, the recommended value for them are: $C_{Rd,c}$ is $0.18/\gamma_c$, k_1 is 0.15. And that for v_{\min} is calculated as:

$$v_{\min} = 0.035 k^{3/2} \cdot f_{ck}^{1/2}$$

The reliability aspect of structure is usually described by probabilistic terms. The reliability required for structures can be achieved by design in accordance with EN 1990 and EN 1999. EN 1990 and EN 1999 introduce the measures relating to design calculation, which are representative values of actions and the choice of partial factors. The representative values, for example, characteristic value, of parameters contain the probability of being exceeded

during the service life. Partial safety factors are introduced to deal with this probability. Combining the representative values with partial safety factors, the design values for material properties, actions and geometry etc. can be derived and used in the design calculation.

Partial safety factor format is a simplified verification concept, which is based on past experience and calibrated in such a way that the general reliability requirements are satisfied with a sufficient margin during a defined period of time (MC 2010). There are three methods introduced in EN 1990: 2002. First, in design codes, partial factors are determined based on the former experience, which is called deterministic methods consisting of historical and empirical methods. Second, one of probabilistic methods, first order reliability methods (FORM) (Level II), make use of certain well-defined approximations and lead to results which for most structural applications can be considered sufficiently accurate (EN 1990: 2002). Third, full probabilistic methods (Level III) can give correct answers in principle but are not used in design codes because this method is based on statistical data. Eurocodes are mainly based on the deterministic methods. The relation between partial factors are shown in Figure 1 where γ_F is partial factor for action and γ_M is for material properties.

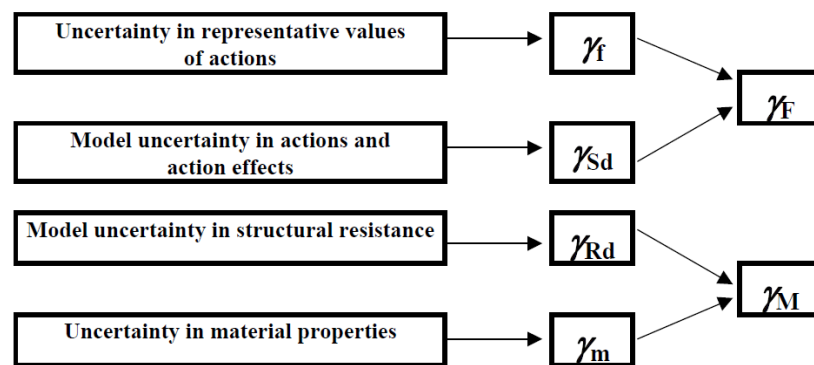


Figure 1 Relation between individual partial factors (Figure C3, EN 1990: 2002)

The partial factors are applied for example, the γ_c to determine empirical factor for characteristic shear capacity.

The safety formats to deal with the uncertainties for non-linear analysis of concrete structure are studied in Schlune *et al.* (2012). New safety formats are developed based on the observation that modelling uncertainties are usually the main factor in safety evaluation. Taking into account the modelling uncertainties of slabs, the proposed safety formats can also be applied in slabs.

In Eurocode, shear design rules for slabs are mostly derived from shear tests on beams and underestimate the shear resistance of one-way slabs. The term σ_{cp} considers the influence of uniaxial force on shear capacity without shear reinforcement. However, the details applied for the case of axial tension force are not addressed (Bui *et al.*, 2017). Thus, this master thesis is supposed to give a better understanding of existing design provision.

2.1.2 ACI 318-14

According to ACI 318-14, chapter 22.5, one-way shear strength, the calculation of shear capacity with axial compression or tension is performed respectively. For non-prestressed members with axial compression, the shear strength is calculated as:

$$V_c = 2 \left(1 + \frac{N_u}{2000A_g} \right) \lambda \sqrt{f'_c} b_w d$$

Note that this formula is the simplified method.

More detailed calculations are:

The nominal shear strength equals the lesser of results of two formula below:

$$V_c = \left(1.9 \lambda \sqrt{f'_c} + 2500 \rho_w \frac{V_u d}{M_u - N_u \frac{(4h-d)}{8}} \right) b_w d$$

And

$$V_c = 3.5 \lambda \sqrt{f'_c} b_w d \sqrt{1 + \frac{N_u}{500A_g}}$$

The first equation only applies when $M_u - N_u \frac{(4h-d)}{8} \leq 0$.

The notions in the equations above are:

V_c is the nominal shear strength provided by concrete

λ is the modification factor, for normal weight concrete, the value is 1

f'_c is specified compressive strength of concrete

$b_w d$ represents the effective cross section area on which the average shear stress is based

N_u and M_u are the factored axial force and moment that occurring with V_u , factored shear

ρ_w is the reinforcement ratio

A_g is the gross area of concrete section

For non-prestressed members with axial tension, the calculation of shear capacity is:

$$V_c = 2 \left(1 - \frac{N_u}{500A_g} \right) \lambda \sqrt{f'_c} b_w d$$

In the calculation, axial compression takes positive while tension goes negative. Notion that the units in ACI follow the American standard, which is f_c' in *psi*, length in *inch* and force in *lb*.

2.2 Numerical assessment method

Finite element method is representative for numerical simulation. When it comes to the design of RC slabs, finite element method is inevitable. Finite element method can deal with the model that has complex geometry and material properties. Linear and non-linear analysis methods are included in finite element method. Non-linear analysis usually produces more accurate results because it considers the non-linear properties of the structure and materials.

Taking into account the nonlinearities, NLFEA is available to lead a better estimation of structural behaviour. There are three main nonlinearities in structural mechanics: material, geometry and contact. And the stiffness matrix varies due to the nonlinearities. Applying the fixed stiffness, the program will lead to the non-equilibrium between internal and external forces. In NLFEA, incremental-iterative procedure is applied to search for the equilibrium. Figure 2 describes the process of NLFEA. Once the difference between internal and external forces is less than the desired tolerance, the program will result in the equilibrium, then iteration will stop. Otherwise the iteration will be repeated until it reaches the maximum steps and non-convergence will be concluded.

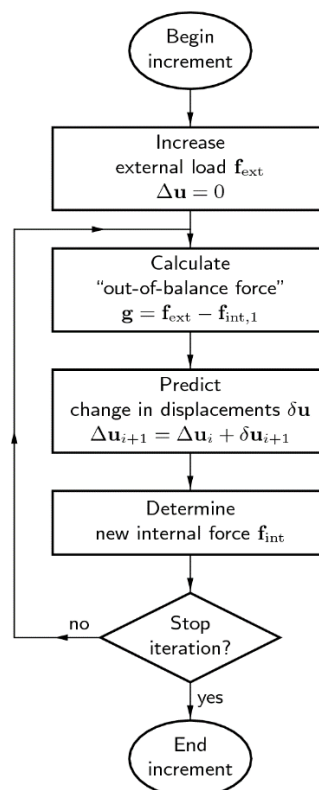


Figure 2 Calculation process of non-linear finite element analysis (Figure 46.1, Diana-10.1 User's Manual, 2017)

When applying NLFEA as a method of assessment, a series of steps have to be taken into account. The Dutch Guideline (Hendriks *et al.*, 2017) gives a set of suggestions to apply NLFEA safely, including the modelling of structures, analysis choices, verification in terms of limit state and the presentation of results. The contents from the Dutch Guideline (Hendriks *et al.*, 2017) related to RC slab without shear reinforcement are summarized in Table 2. Notion that Dutch Guideline (Hendriks *et al.*, 2017) proposed a recommendation of presentation of NLFEA results. It contains the method that how to apply the NLFEA to finish an assessment, which includes five steps: specification, model preparation and checking, analysis, validation and post-analysis checks. A similar process is presented by Engen (2017). The author uses the term *solution strategy* to describe choices that need to be made in a NLFEA (Engen, 2017). Table 1 shows the idea.

In this master thesis, the numerical assessment will be carried by nonlinear finite element analysis using TNO Diana. And the modelling will refer to the Dutch Guideline (Hendriks *et al.*, 2017) and the results from Nana *et al.* (2017).

Table 1 The activities in the process of developing a solution strategy for NLFEA (Engen, 2017)

Definition	Select suitable material models, element types, iteration methods, etc.
Verification	Apply fundamental checks to assess if the model works as expected and assess the sensitivity to variations of the solution strategy, e.g. mesh size sensitivity and load step size sensitivity.
Validation	Assess how well the NLFEA predictions compare to the real structural behaviour, i.e. quantifying the modelling uncertainty by comparing NLFEA predictions to experimentally obtained results.
Demonstration of applicability	Prove that the solution strategy is suitable for the intended purpose.

Table 2 Summary of the Dutch Guideline (Hendriks *et al.*, 2017) that related to this master thesis

modelling	material	concrete	material parameters: based on MC2010 total strain-based crack model (fixed & rotating): <ul style="list-style-type: none"> tensile behaviour: softening model shear behaviour: shear retention model, only for fixed compression behaviour: softening model multi-axial load interaction crack-band width: element dimension or mean crack distance
		steel reinforcement	material parameters: based on MC2010 interaction between reinforcement and concrete: <ul style="list-style-type: none"> tension-stiffening bond-slip relation: fully-bonded assumption is sufficient dowel action
	element discretization	concrete	3D slab modelling: solid element <ul style="list-style-type: none"> quadratic 20-node hexahedron quadratic 20-node tetrahedral
		steel reinforcement	2D reinforcement bar: truss element
		element size	minimum size: no minimum size requirement maximum size: reach relatively smooth stress field
	Load	force	
		displacement	more stable than force control in certain cases
	Boundary condition	support	
		load plate	distributed concentrated force
		interface	between plate and concrete
symmetry		symmetric failure mode, reduce computational costs	
analysis	load incrementation		0.5 of the load of first crack based on nonlinearity behaviour
	equilibrium iteration		Newton-Raphson with arc-length control
	convergence criteria	unbalanced force norm	tolerance recommended: 0.01
		displacement norm	
energy norm		tolerance recommended: 0.001	
Limit state verification	ultimate limit state (ULS)	Global Resistance Factor Method (GRF)	MC2010
		Partial Safety Factor Method (PF)	
		Estimation of Coefficient of Variation of Resistance Method (ECOV)	

2.3 Multi-level assessment method

2.3.1 Concept of multi-level assessment

Multi-level assessment is a method that integrates analytical and numerical methods. It studies the accuracy of outcomes from different methods and relates the outcomes to the cost of each method. Based on this knowledge, recommendations are given that which assessment method can be applied in specific design phase. Multi-level assessment is a global view of the application of analytical and numerical methods.

Model Code 2010 introduces the concept of Levels-of-Approximation (LoA), which is a design strategy where the accuracy of the estimate of a structural member's response (behaviour or strength) can be, if necessary, progressively refined through a better estimate of the physical parameters involved in the design equations (Model code 2010). This means that the assessment of structures is integrated according to their accuracy and time or labour consumption. With higher level, the better estimation of structural response is, the longer time is devoted to the performance. Figure 3 describes this relation.

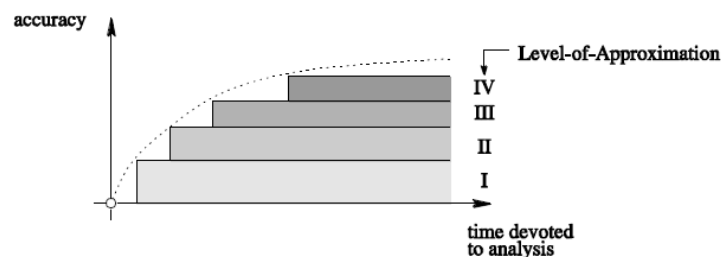


Figure 3 Accuracy on the estimate of the actual behaviour as a function of time devoted to the analysis for various Levels-of-Approximation (Figure 3.1-1, MC2010)

The first LoA is based on simple and safe hypothesis that evaluating the physical parameters of design equations. This level leads to a safe estimation of structural behaviour with low time consumption. Thus, this level is usually sufficient for preliminary design phase. Further analytical and numerical study in successive LoA method can refine the parameters. In the meantime, more time and labour is devoted to the study.

The Level II and III successively refines the parameters to give a more accurate estimation. Their application is advised for the tender and final design of new structures as well as for the assessment of existing structures.

It is stated in Model Code 2010 that numerical analysis gives the best estimation of structural response. They are always in the highest level of LoA. However, this method costs more time and labour. Model Code 2010 advises that numerical analysis should be used for the final design of very complex structures or for the assessment of critical existing structures. This is justified when a more accurate estimation of the physical parameters can lead to significant savings by avoiding or limiting strengthening of the structures. (Model Code 2010)

In terms of RC slabs, Shu (2017) proposes a methodology for successively improved structural analysis for the assessment called Multi-level Assessment Strategy in his Doctor Thesis, *Structural Analysis Methods for the Assessment of Reinforced Concrete Slabs*. This method

focuses on the structural analysis of the slab and connects structural analysis with resistance models at different levels in Eurocode 2 and MC2010. (Shu, 2017) The method divides the structural analysis into five levels. Higher the level is, more accurate results can be obtained and more time and skill is needed. According to Shu (2017):

- Level I is defined as simplified analysis methods, for example, the code provisions and simplified mechanical models.
- Level II is 3D linear FE analysis, assuming linear elastic behaviour to be able to superimpose the effect of different loads, to achieve the maximum internal forces throughout the structure for all possible load combinations. The results should be compared with the local structural analytical results. In this phase, non-linearity is not considered. Thus, the results are not able to show the structural behaviour before the maximum internal forces.
- Level III is defined as 3D non-linear shell FE analysis with fully bonded reinforcement. It is used to reflect the flexural strength of RC slabs directly in FE analysis. However, at level III, the out-of-plane shear strength, such as punching shear failure, is missed due to the property of shell element.
- Level IV is 3D non-linear FE analysis with continuum elements coupled with fully bonded reinforcement. The short come of this phase is that bond strength and its effect on shear failure should be verified separately.
- Level V refines the Level IV to additionally modelling the bond-slip effect between reinforcement and concrete. This method can give more accurate estimation and reflect better structural behaviour. No more failure modes need to be checked separately.

It is necessary to note that an improvement, in other words, a more precise assessment is proof loading. If none of the analytical methods lead to satisfactory results, but there are possible sources for additional capacity in the structure, a proof load test can be considered (Lantsoght *et al.*, 2017). The stop criteria are studied which indicate the termination of proof loading and the assessment of desired capacity of specific structure. And a Guideline for proof loading is in process. In this master thesis, the main topic is about the numerical assessment, proof loading will not be discussed and applied to objective structures.

2.3.2 Comparison of experimental, analytical and numerical results for RC slabs

As is mentioned, non-linear finite element analysis of slabs can estimate the strength accurately and lead to a better understanding of structural behaviour compared to linear finite element analysis. This is because the assumption of linear elastic material behaviour of concrete structures can lead to a modelled structural response and internal force distribution that deviates significantly from reality. It becomes necessary and important to investigate the accuracy and reliability of NLFEA. Several series of research on RC slab without shear reinforcement have been reported. Researchers test RC slabs to get the experimental samples. Analytical and numerical assessments have then been applied on the tested slabs. The outcomes are compared and analysed. In this chapter, three series of research will be included: 1) Lantsoght *et al.* (2013) & Belletti *et al.* (2014); 2) Shu (2017); 3) Bui *et al.* (2016) & Nana *et al.* (2017).

Lantsoght *et al.* & Belletti *et al.* & Hendriks *et al.*

The experiment of 38 slabs under a concentrated load close to the support has been reported in Lantsoght *et al.* (2013), with various width, reinforcement layout, concrete strength and size of loading plates. In terms of the analytical assessment, the calculation is done by authors based on both EN 1992-1-1:2005 and ACI 318-08. In addition, the French National Annex combined with factor β and the method from Regan are also applied in analytical assessment.

The comparison of experiments, analytical assessment and numerical assessment is done by Belletti *et al.* (2014). Three slabs are chosen from Lantsoght’s experiments, named S1T1, S1T2 and S4T1. The ultimate load of three slabs obtained from various assessment is shown below. Notion that the Level I and Level II assessment are based on the shear calculation in MC2010.

Table 3 Ultimate load (in kN) of slabs S1T1, S1T2 and S4T1: experimental results and calculated results obtained with the actual mechanical properties of the materials. (Belletti *et al.*, 2014)

Exp.	Analytical calculations						NLFE analyses		
	One-way shear failure	One-way shear		Punching			Bending Yield line	Shell model	Brick model
		Level I	Level II	Regan	EC2	CSCT			
S1T1	954.0	307.3	536.5	708.2	698.1	793.0	1970.5	1811.8	906.1
S1T2	1023.0	242.4	734.1	708.2	698.1	-	-	-	1020.1
S4T1	1160.0	344.6	559.4	769.0	952.6	-	-	-	883.1

A specific study of the LoA is presented according to MC2010. Only Level I, II and IV are performed to find the design shear strength of structure without shear reinforcement in ULS, within which Level I is derived from the more general Level II Approximation with the assumption that the mid-depth strain at the control section can be taken as $\epsilon_x = 0.00125$, which corresponds to half the yield strain for a reinforcing bar with $f_k = 500MPa$ ($\epsilon_x \approx f_{yk} / (2E_s)$) (fib, 2013). The Level IV is with NLFEA with brick elements and three alternative safety formats, partial factor (PF), global resistance factor (GRF) and estimation of coefficient of variation of resistance (ECOV) are applied. The results of MoA that comparing with experiments and NLFEA without safety formats are shown below.

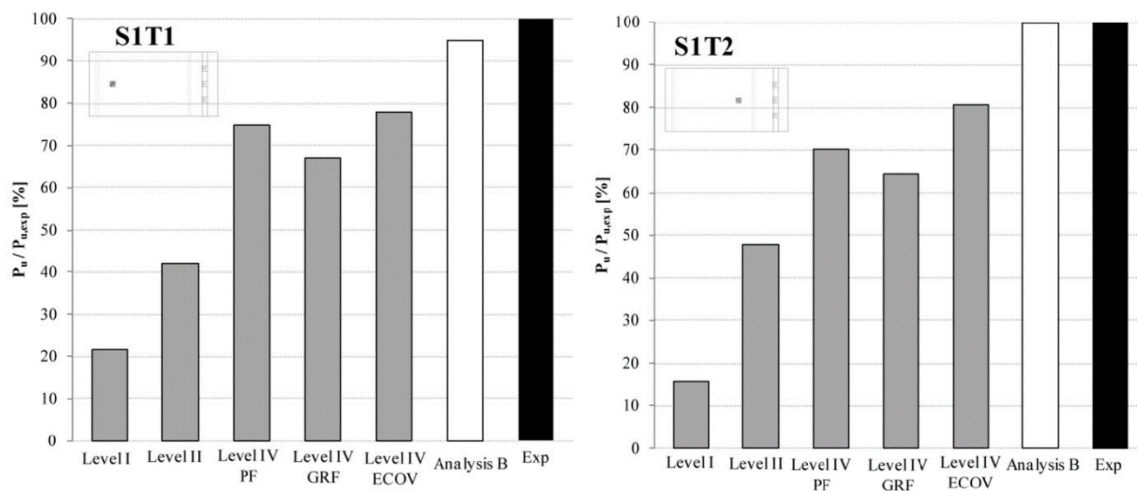
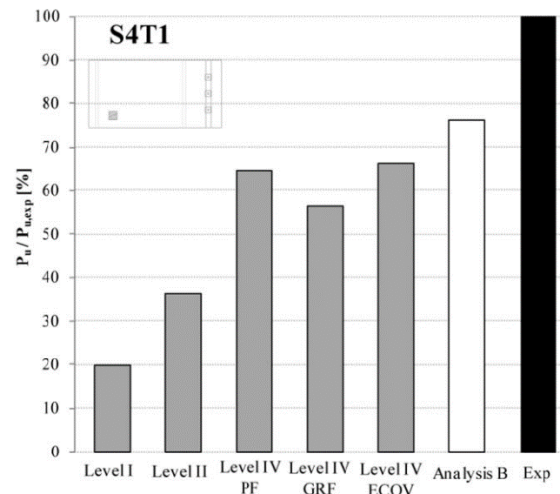


Figure 4 Ultimate design loads P_u obtained analytically and numerically as a ratio of the experimental result $P_{u,exp}$ (exp.). (Figure 13, Belletti *et al.*, 2013).



Continue of Figure 4

Notion that Analysis B is the NLFEA without safety formats using actual mechanical properties (Belletti *et al.*, 2013). The full comparison of experimental, analytical and numerical results is reported in the Validation of Dutch Guideline (Hendriks *et al.*, 2017) as well.

Shu

In Shu (2017), the multi-level assessment proposed by the author is applied two case studies: two-way slabs subjected to bending and a cantilever slab subjected to shear. The experimental setup is described in Shu (2017). The calculation methods are listed in the Table 4.

Table 4 Applied analysis methods for two-way and cantilever slabs at different assessment levels. (Shu, 2017)

	Two-way slab	cantilever slab	Procedure
Experiment			
Level V	Non-linear continuum FE analysis with bond-slip reinforcement		One-step
Level IV	Non-linear continuum FE analysis with fully-bonded reinforcement		One-step
Level III	Non-linear shell FEA	Non-linear shell FEA + MC2010	Two-step
Level II	Linear shell FEA + MC2010	Linear shell FEA + MC2010	Two-step
Level I	Eurocode 2	Eurocode 2	Two-step

And the bending and shear capacity from different assessment levels and experimental results are shown in Figure 5. It is apparent that the capacity increases for higher level but cannot exceed the experimental results.

In addition, Shu (2017) also applies the multi-level assessment on an existing bridge deck slab, emphasizing the results comparison between multi-level assessment and field test. The field test is carried out on a 55-year-old existing RC bridge deck slab under concentrated load near the girder (Shu, 2017). Because that the research is based on laboratory experiment in this master thesis, the study of comparison between multi-level assessment and field test will not be included.

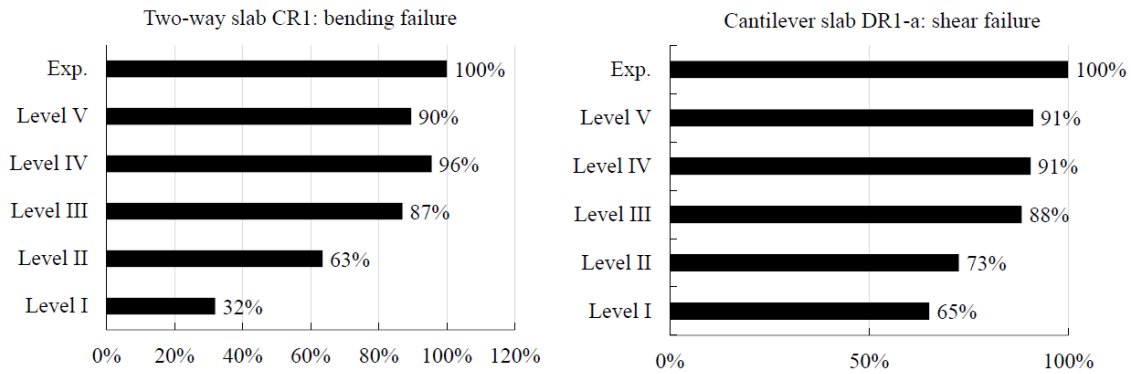


Figure 5 Load capacity of a two-way and a cantilever slab at different levels (Figure 26, Shu, 2017)

Bui *et al.* & Nana *et al.*

In Bui *et al.* (2016), ten tests on seven RC slabs without shear reinforcement are performed. The slabs are simply supported on four sides and loaded in concentrated force near support. Analytical methods are performed on these slabs according to EN 1992-1-1:2005, Eurocode with French national approach, extension of Eurocode shear formula proposed by Lantsoght *et al.* (2015), ACI 318-14 with and without simplified methods. The comparison between experiments and analytical calculation is shown in Figure 6.

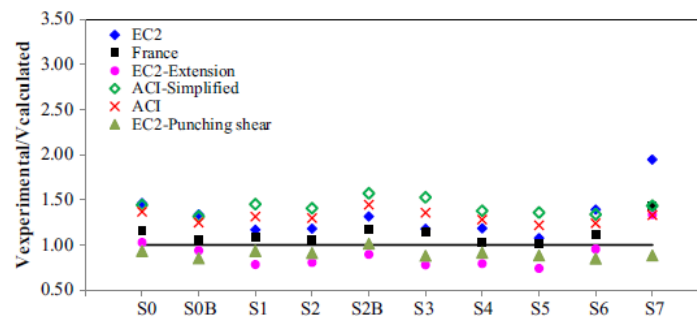


Figure 6 Comparison of tests and analytical calculation (Figure 16, Bui *et al.*, 2016)

In Nana *et al.* (2017), ten tests on 9 slabs are done. These slabs are also loaded in concentrated force near support and have no shear reinforcement. Seven slab tests studied in Nana *et al.* (2017) are also included in Bui *et al.* (2016), named S1, S2, S2B, S3, S4, S5 and S6. NLFEA is applied to simulate these slabs and the comparison is performed between experiments and numerical assessment. Notion that the safety formats are not applied in the NLFEA.

It is obvious that the assessment of slabs can contain three parts: experiment, analytical assessment and numerical assessment. The methodology contains in the studies mentioned above is that the validation of analytical and numerical assessment should be based on specific experiments on specific slabs. Through this, the application of assessment methods on RC slabs in various condition can be studied. This thesis is supposed to use the analogous method to study the RC slab without shear reinforcement loaded in out-of-plane concentrated load near support and in-plane compression or tension.

3. Case study of slab without in-plane load

In this chapter, case study of slab without in-plane load is introduced in three parts. First, the experiment by Bui *et al.* (2017) is introduced that one RC slab loaded in vertical out-of-plane force without uniaxial in-plane force (S2). Second, the nonlinear finite element modelling of S2 performed by Nana *et al.* (2017) is described. Third, the nonlinear finite element modelling is applied on this slab by using Diana. Then, the results of NLFEA of this thesis is presented and discussed.

3.1 Experiment by Bui *et al.* (2017)

3.1.1 Material

Concrete C20/25 with the maximum aggregate size of 11.2 mm. The compressive strength corresponding to the mixture used for the specimens is identified from the cylinder compression tests measured on the day the slabs are tested. The modulus of elasticity and the tensile strength are experimentally obtained in the testing day. The slab properties are shown in Table 5.

Table 5 Slab properties of slab without uniaxial in-plane load

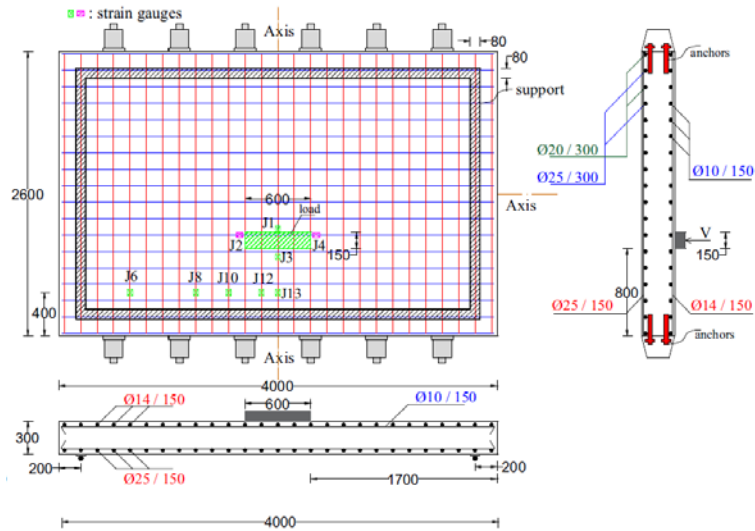
Slab	Axial load (kN)	Axial stress (MPa)	$f_{cm,cyl}$ (MPa)	$f_{ctm,cyl}$ (MPa)	Young's modulus (GPa)	Specimen age at testing
S2	0	0.0	30.9	2.9	31.75	46

Reinforcements use FeE 500B. Properties of reinforcement follow the standard and are not measured in the testing day. The deformed bars are standard ribbed bars with different diameters. The concrete cover is set as 20 mm for the longitudinal reinforcement. The reinforcement ratio is $\rho_l = 1.223\%$ in longitudinal direction and $\rho_t = 1.106\%$ in transverse direction respectively.

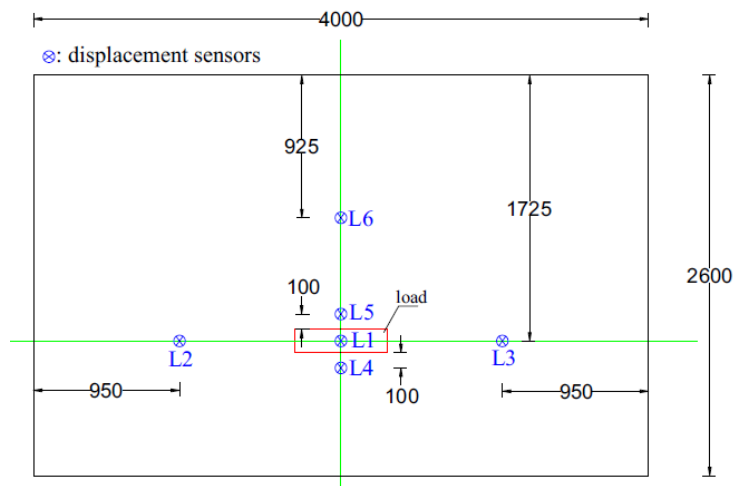
There is no shear reinforcement in slab.

3.1.2 Geometry

The dimension of slabs is 4 m x 2.6 m x 0.3 m. A loading plate is positioned near support. The thickness of the loading plate is not given. Therefore, the thickness will be chosen following the element size. Figure 7 shows the slab and reinforcement layout. In addition, the displacement sensor and strain gauges' position is shown as well.



(a)



(b)

Figure 7 a) Slab dimension and reinforcement layouts; b) Position of displacement sensors. (Figure 1, Bui *et al.*, 2017) [mm]

The ratio a_v / d_t is noticed as an important parameter to influence the shear capacity of RC slabs. In this experiment $a_v / d_t = 2.1$, where a_v is the distance between edge of loading plate and edge of support steel plate, and $d_t = 267.5\text{mm}$ is the effective depth to the longitudinal reinforcement. Figure 8 shows the position of a_v .

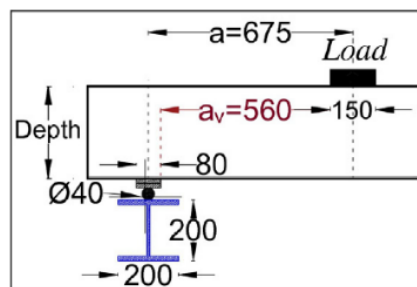


Figure 8 Position of a_v , side view in transverse direction (Figure 3, Nana *et al.*, 2017) [mm]

3.1.3 Boundary condition

Slabs are simply supported on four sides. According to Nana *et al.* (2017), the support system consists of three parts: first, a 200 by 200 steel I-beam is laid on the slab of the test hall. A round bar 40 mm in diameter is then positioned above the steel beam. A metallic plate measuring 80 by 12 mm is placed between the round bar and slabs. Before positioning the slabs on the support, an approximately 4-mm-thick bed of mortar was placed above the steel plate, at the interface between the supports and the slab, to ensure regular contact and ensure the uniformity of the support. The support system can be described in the Figure 9.

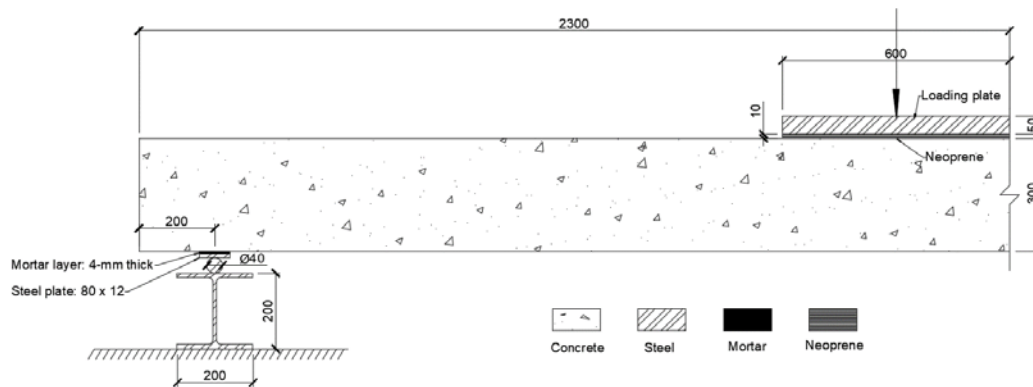


Figure 9 Support system. (Figure 4, Nana *et al.*, 2017) [mm]

3.1.4 Loading method

The vertical load is applied by one out-of-plane hydraulic jack, with maximum load capacity of 2000 kN. The out-of-plane load is distributed by a rectangular steel plate measuring 600 mm by 150 mm. The same series of tests are also reported in Nana *et al.* (2017) where more details of test setup can be found. According to Nana *et al.* (2017), a layer of 10-mm neoprene is in between load plate and slab surface to distribute load.

3.1.5 Experimental results

Three kinds of cracks are observed and indicated in Bui *et al.* (2017). First, the flexural cracks parallel or perpendicular to the supports are located at the same locations of bottom reinforcement. Second, two-way shear cracks also occur that is indicated as a perimeter surrounding loading area at the bottom of the slab. However, the failure is not caused by the punching shear mechanism. The third cracks, which causes the final failure, is the pure one-way shear that is indicated by the cracks near the steel support. The Figure 10 shows the failure modes of S2 that is without uniaxial force in experiment.

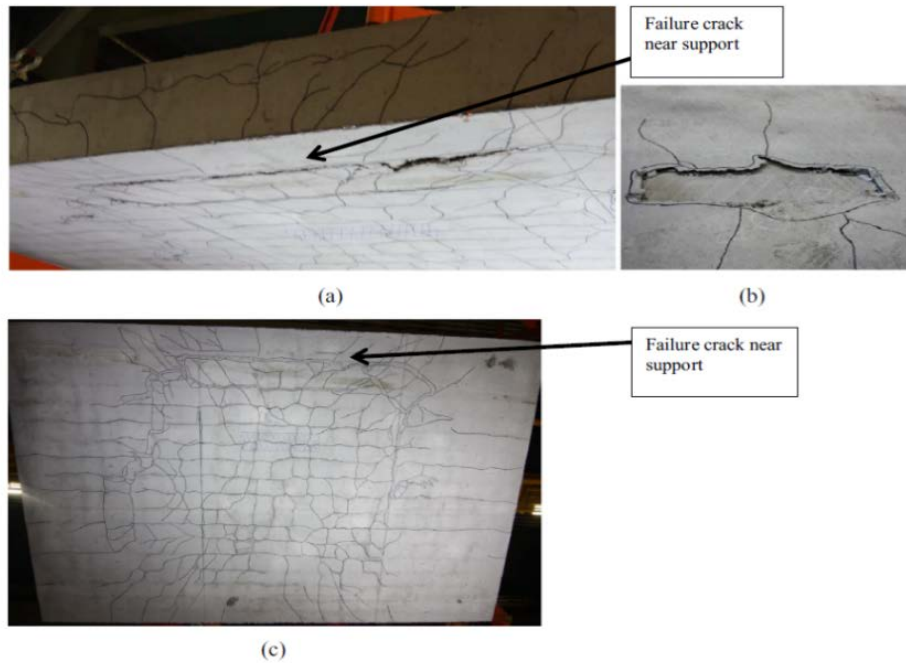


Figure 10 Shear failure observed of slabs S2 (Figure 6, Bui *et al.*, 2017)

The cracking indication of slab loaded without uniaxial in-plane load (S2) is shown in Figure 11.

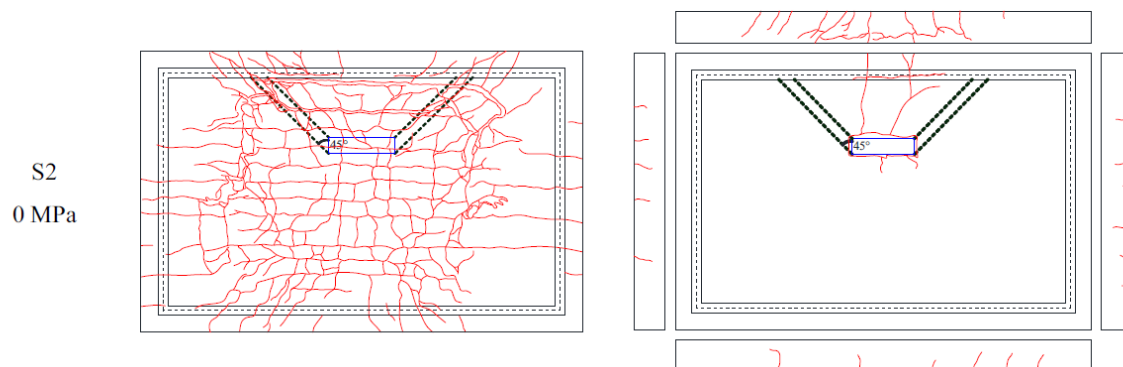


Figure 11 Cracks indication (Figure 7, Bui *et al.*, 2017)

Based on the experimental results, the relation between shear load and displacement at L5 of slab S2 is shown in the Figure 12. Note that the shear load is calculated according to Navier solution obtained for simply supported rectangular plate with linear displacement hypothesis. (Limam *et al.*, 2017). This method is presented in Timoshenko *et al.* (1959). The shear load is assumed to be distributed over the effective width which is determined as 45° from the far corner of loading plate. In this chapter, the structural behaviour is mainly discussed on S2, other slabs have similar behaviours. The ultimate load that S2 takes is 1220 kN. Then the shear load that calculated from ultimate load is 747 kN. At peak load, the displacement is measured at the LVDT of L5 near the loading plate, which is 4.62 mm.

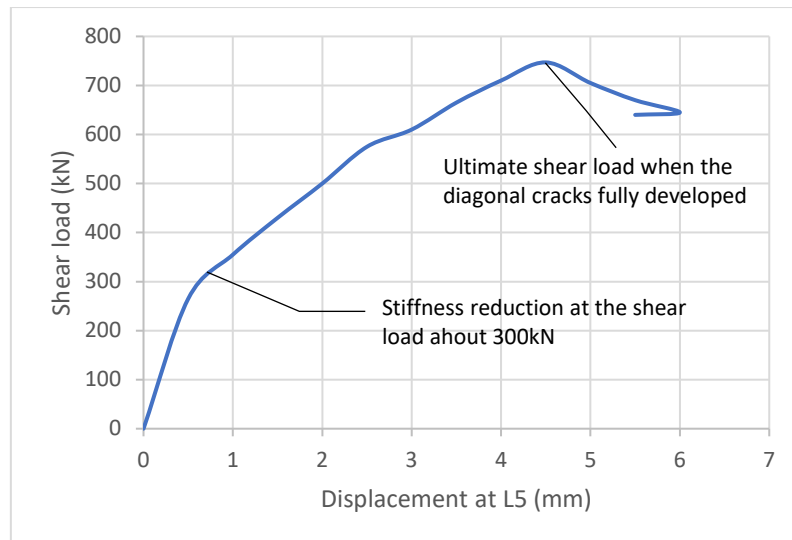


Figure 12 Shear load - displacement curve for S2

The development of crack can be described in such order:

- In S2, the first crack is monitored by J1 (located at the bottom layer of longitudinal reinforcement) when the elongation slope changes. The initial crack is flexural crack due to the bending under loading plate at about 125 kN.
- The crack in transverse direction is detected by J2 and J4 (located at the bottom layer of transverse reinforcement under loading plate) at about 290 kN. This indicates that the punching shear is formed.
- When the concentrated load reaches about 461 kN, J12 and J13 (located at the bottom layer of longitudinal reinforcement near support) detect the slope changing. This is the deformation due to diagonal tension crack developed from the edge of loading plate to the bottom of slab.
- The failure crack along the support edge is developed at about 750 kN. This indicates the failure of structure is caused by one-way shear.

The shear loading and strain relation is plotted in the Figure 13.

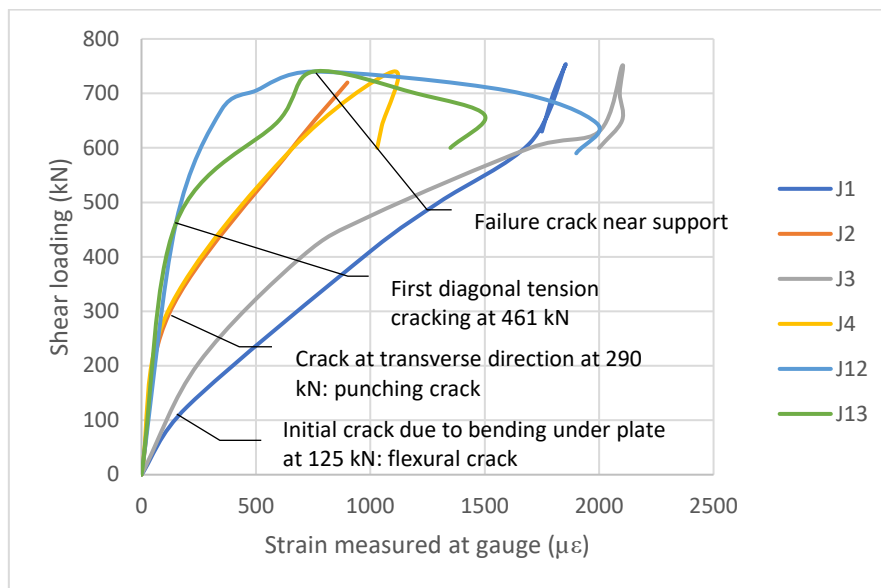


Figure 13 Shear load strain curve for S2

3.2 Nonlinear finite element model on S2 by Nana *et al.* (2017)

3.2.1 Overview

The S2 slab (without uniaxial load) is modelled by Nana *et al.* (2017). This numerical research is conducted using the FEM software Abaqus. An explicit quasi-static solution technique in Abaqus/Explicit is used to reduce the convergence problems due to the stiffness reduction when concrete cracks and fails by shear, although explicit methods require very small time increments to satisfy the stability limits (Nana *et al.*, 2017). The concrete is modelled using concrete damage plasticity (CDP) model.

3.2.2 CDP model

There are two main phenomena to characterize the mechanical behaviour of concrete in the strain-softening branch: the reduction in elastic stiffness and the development of irreversible strains (Nana *et al.*, 2017). As pure damage model, using an unloading slope to reproduce the reduction of elastic stiffness is always passing through the original one. Therefore, the damage value is overestimated. In terms of the pure plastic model, it cannot reproduce the reduction of characteristic stiffness, then the strain value is overestimated. The CDP model takes into account the plasticity and damage, the outcome can be more accurate when combining these two model's advantages.

The CDP model can capture the concrete behaviour such as elasticity, hardening and softening. However, the particular attention is given to the simulation of the strain-softening branch of the stress-strain uniaxial behaviour curves (Nana *et al.*, 2017). This model uses isotropic damage approach with isotropic tensile and compressive plasticity to represent the inelastic behaviour of concrete (Nana *et al.*, 2017).

CDP model is a smeared crack model, which means that the nodes, on the contrary of discrete crack model, will not separate during the cracking process. The crack area is related to the

element size. The tensile fracture energy G_f is calculated following Model Code 1990 and Model Code 2010 respectively. Other parameters calculation in this numerical research will not be stated here because different FEM software is used in this master thesis and more information can be found in Nana *et al.* (2017).

3.2.3 Modelling description

According to Nana *et al.* (2017), only half of the slab is modelled to decrease the calculation time and better convergence due to the symmetry in the transverse direction. The model is built in 3D with continuum elements. The concrete region is meshed by eight-node hexahedral elements (C3D8R) with a reduced integration scheme to avoid the shear locking effect [28], and the reinforcements were meshed by two-node linear beam elements (B31) (Nana *et al.*, 2017). Reinforcement are fully bonded within concrete. Mesh size is determined as 20 mm through a mesh convergence study. The slab is simply supported around all four sides by modelling four rigid supports. The mortar layer between steel support plate and concrete slab is ignored in the model. The vertical load is applied on the entire surface of the loading plate and the increment is with displacement control. The Figure 14 shows the model of this slab.

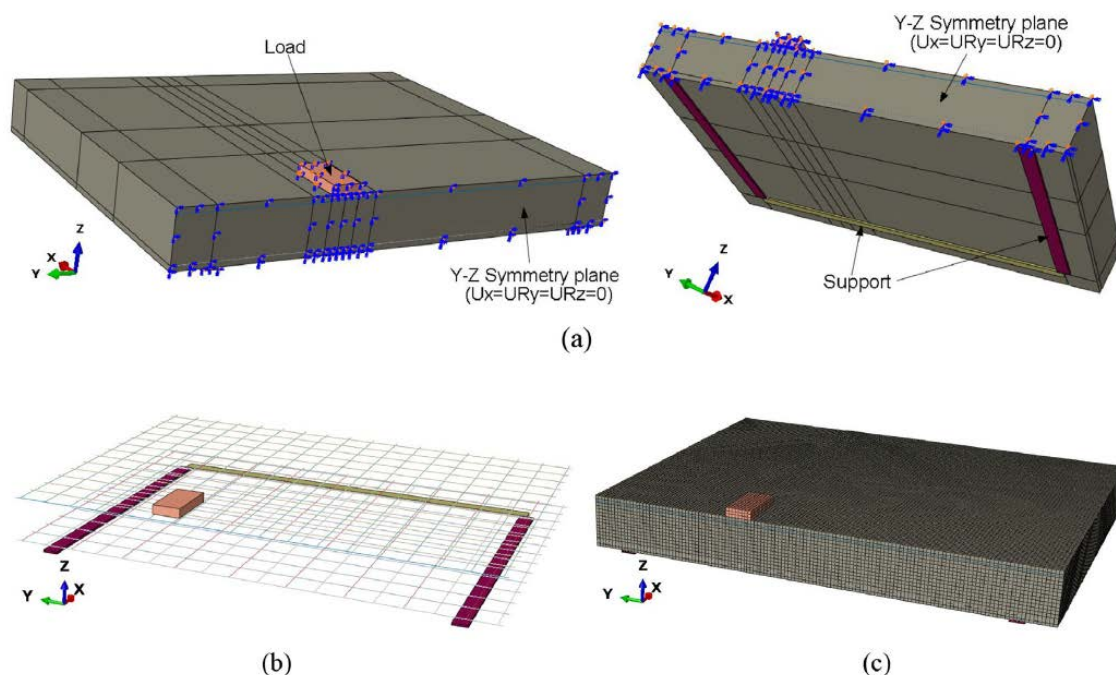


Figure 14 Model of the slab: a) Geometry and boundary conditions; b) Reinforcement layout; c) Finite element mesh (Figure 14, Nana *et al.*, 2017)

3.2.4 Results and discussion

The shear load – displacement figure from the NLFEA is shown below. The shear load in the figure is calculated according to Navier solution obtained for a simply supported rectangular plate with linear displacement hypothesis (Limam *et al.*, 2017). The displacement is the vertical displacement at L5 which is indicated in Figure 15. From this figure, it can be observed that the initial elastic stiffness of NLFEA is similar with the experiment result. After cracks developed, the stiffer behaviour in the crack formation stage in NLFEA occurs. During this process, the stiffness of slab decreased gradually in both NLFEA and experiment. When failure

of structure is reached, NLFEA shows a close ultimate load to experiment. However, the vertical displacement at failure in NLFEA is less than the experiment. According to Nana *et al.* (2017), there is a layer of 4-mm mortar that can ensure a good contact between steel plate and concrete slab. This support system and mortar layer will deform under vertical load and can increase the total displacement of slab. In the numerical modelling, the mortar is not taken into account. Thus, this could explain why the stiffness predicted by the numerical modelling is stiffer than the experiment results.

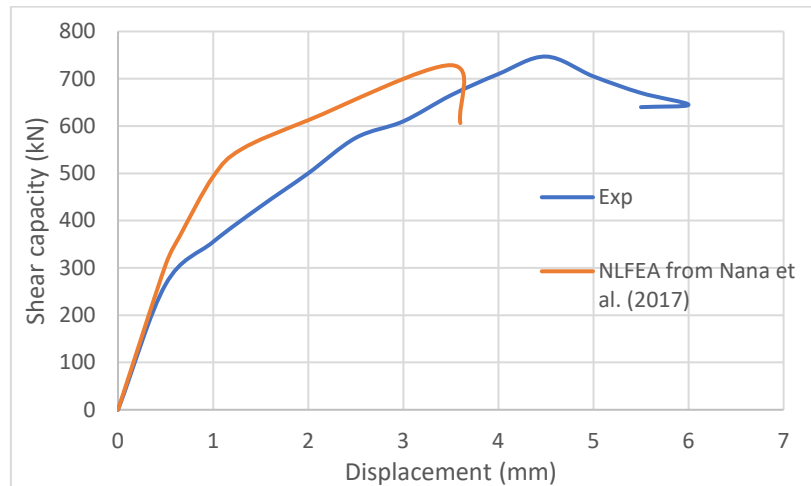


Figure 15 Shear load – displacement relation

When it comes to the crack pattern, the cracks are visualized through the maximum principal plastic strains in the numerical modelling. Compared to the crack patterns observed in the experimental tests, the proposed non-linear FE model shows an accurate prediction of the locations and the directions of the crack propagations (Nana *et al.*, 2017). The cracking pattern at ultimate load visualized through the maximum principal plastic strains is shown in Figure 16. And, however, it can be seen from this figure that the slab in NLFEA is failed more likely in punching shear rather than one-way shear. The reason behind this phenomenon is not discussed in this numerical modelling.

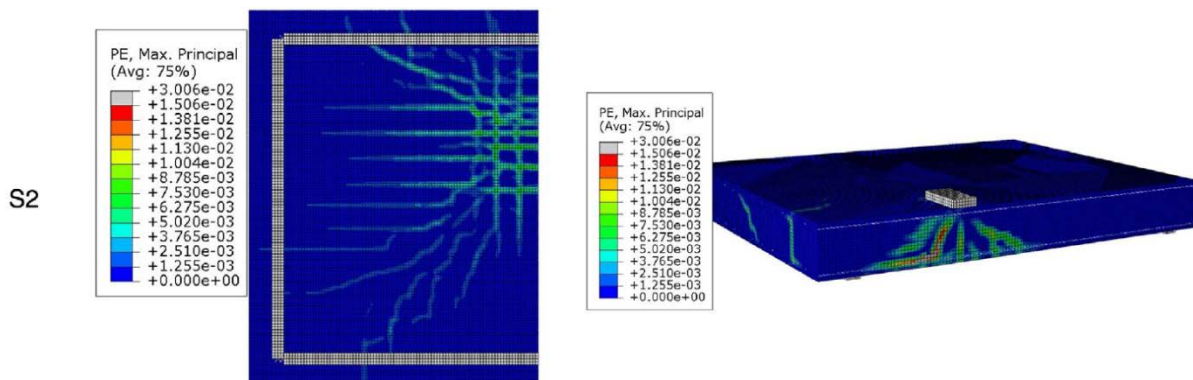


Figure 16 Cracking pattern at ultimate load visualized through the maximum principal plastic strains (Figure 20, Nana *et al.*, 2017)

When comparing the ultimate load from experimental results, numerical modelling and the design codes (EN 1992-1-1: 2005), conclusion can be made that prediction from FEM is less conservative compared to the design code. Consequently, the FEM predictions are more

accurate. Nevertheless, the design codes can predict the shear capacity of slabs with a reasonable safety margin (Nana *et al.*, 2017). The Figure 17 shows the comparison results of ultimate load ratio. Note that the vertical axis is the ratio between ultimate load rather than calculated shear load. Other slabs rather than S2 will not be introduced in this section because the only interesting slab for this master thesis is S2. Even though, the comparison results of all slabs are valuable and can also be referred to by this master thesis.

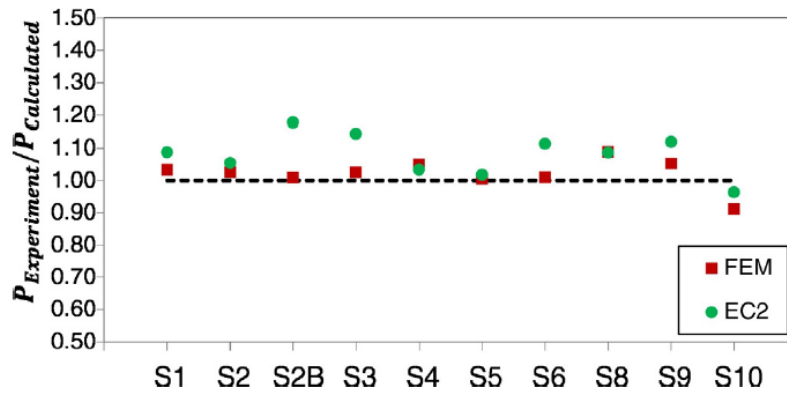


Figure 17 Comparison of the experimental, numerical (FEM) and analytical (EC2) ultimate load for all slabs (Figure 17, Nana *et al.*, 2017)

In addition, other researches and discussions such as the parametric study are stated in Nana *et al.* (2017). But these contents will not be included in this section. Only the related parts are selected and re-described.

3.3 Modelling assumptions

3.3.1 Material

The material parameters will be calculated according to the Dutch Guideline (Hendriks *et al.*, 2017). The concrete is simulated by applying fixed total strain-based crack model for constitutive models. The tensile behaviour is expressed as exponential curve, the poisson ratio reduces based on damage. Compression behaviour is modelled as parabolic curve and reduction model is from Vecchio and Collins 1993. Shear retention is damage based. The reinforcement (FeE 500B) is simulated as ideal plasticity model ($f_{yk} = 500MPa$). There is no hardening behaviour for reinforcement. The reinforcement is embedded, which means that the fully-bonded relation between reinforcement and concrete. The constitutive model of concrete and steel is shown in Figure 18.

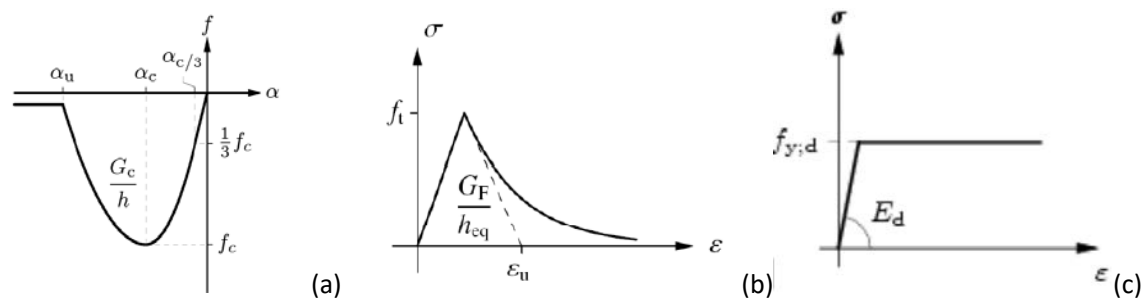


Figure 18 Constitutive model: a) Parabolic curve for concrete in compression; b) Exponential curve for concrete in tension; c) ideal plasticity curve for steel. (a: Figure 6.6, b: Figure 6.4, c: Figure 10.3, Diana-10.1 User's Manual, 2017)

3.3.2 Boundary conditions

In the experiments, the slabs are simply supported on four sides. According to Nana *et al.* (2017), the boundary conditions are simulated as four rigid supports. Due to the relative complexity of the support system, rational simplification is necessary for 3D modelling of slabs to reduce the analysis cost. Thus, the simplified scheme of support system can be explained in the Figure 19.

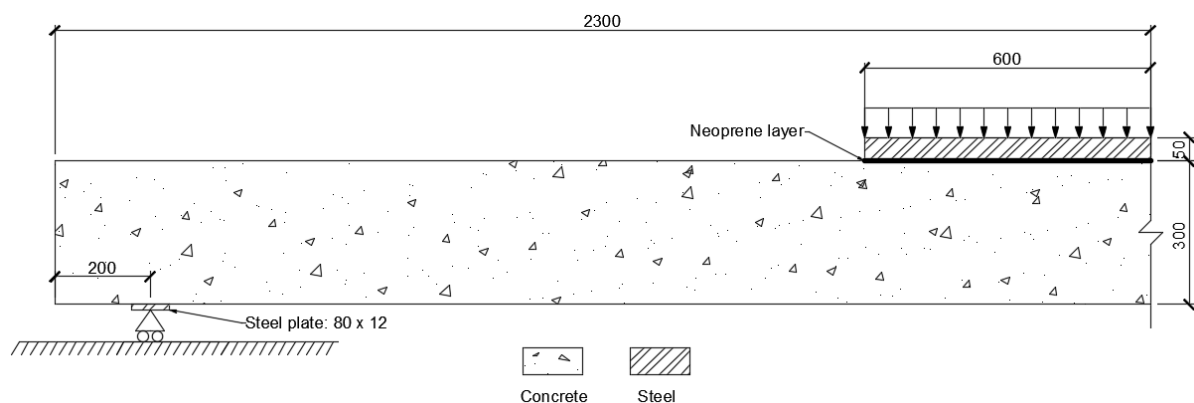


Figure 19 Simplified scheme of experimental slabs. Unit: [mm]

The mortar layer between slab and steel plate is ignored. Here are two reasons to name. First, the purpose in the experiments to position mortar layer is to ensure regular contact and

ensure the uniformity of the support. In reality, the contact between slab and steel plate cannot be perfect, however, the surface of slab and steel plate is perfectly plane in the modelling. Thus, it is not necessary to apply the bed of mortar in between.

Second, according to the experimental results, the ultimate load is 1200 kN. Assuming that the reaction force is uniformly distributed along support. The area of support steel plate is:

$$A = 2 \cdot w \cdot (l_l + l_t) = 2 \times 80 \times (3520 + 2200) = 915200 \text{ mm}^2$$

Where:

w is the width of steel plate of support;

l_l and l_t are the length of steel plate of support in longitudinal and transverse direction.

The scheme of steel plate of support is depicted:

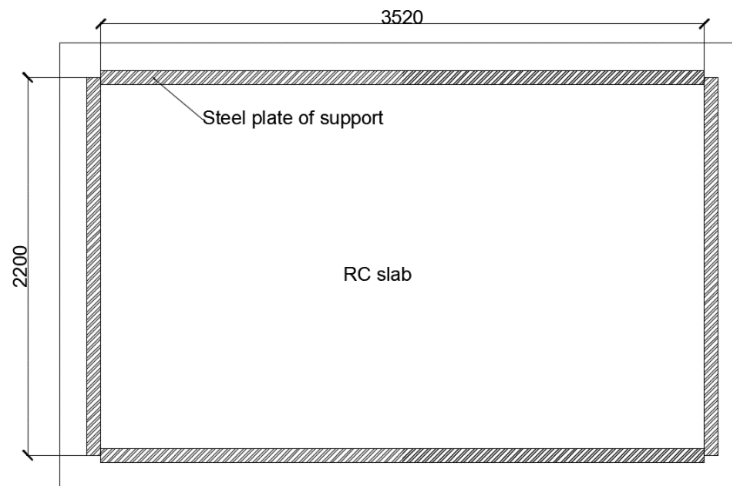


Figure 20 Scheme of steel plate of support [mm]

Thus, the compressive stress on the support is:

$$\sigma_c = \frac{1200 \text{ kN}}{2 \times 80 \times (3520 + 2200) \text{ mm}^2} = 1.3 \text{ MPa}$$

The strain of mortar layer due to compression is:

$$\varepsilon_c = \frac{\sigma_c}{E_{\text{mortar}}} = \frac{1.3}{3851} = 0.034\%$$

Where the young's modulus of mortar is $E_{\text{mortar}} = 3851 \text{ N/mm}^2$, assuming normal cement mortar is applied. The deformation of the mortar is:

$$\Delta t_m = t_m \cdot \varepsilon_c = 4 \times 0.034\% = 1.35 \times 10^{-3} \text{ mm}$$

This deformation in vertical direction is too small compared to the structural deformation at

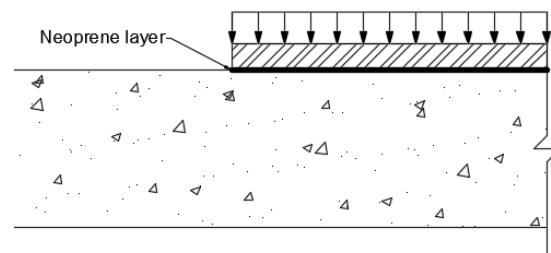
ultimate load stage, which is about 4.5 mm as is shown in Figure 8. Thus, the layer of mortar can be ignored.

3.3.3 Out-of-plane loading

From Figure 21 it can be found that the out-of-plane load is applied on part of the top surface of loading plate. Then this load will be distributed by the loading plate and the neoprene. In mechanical model, this load is simplified as a distributed load applied on entire top surface of loading plate.



(a)



(b)

Figure 21 a) Out-of-plane load in experiment (Figure 2, Nana *et al.*, 2017); b) Out-of-plane load in mechanical model

3.4 Modelling choices

The modelling of RC slab contains several aspects: material and element, boundary conditions, loading methods, NLFEA method. In this chapter, these aspects will be presented respectively. The reason for the modelling choices will also be introduced.

3.4.1 Material

In 3D modelling, solid element is applied for concrete. Truss element is used for reinforcement. A layer of neoprene is modelled as solid element even though the thickness of neoprene is relatively small compared to element size. Ignoring the mortar layer between supporting steel plate and concrete changes the behaviour around four corners of slab. Because corners of slab uplift during the loading process. Nevertheless, perfect connection between steel plate and concrete is modelled without mortar layer in numerical model. Thus, an interface is set on top of supporting steel plates. It is assumed that a 1-mm-thick steel layer as 3D interface. Discrete cracking model is applied so that once there is tension concrete and steel plate would divide. In this way, the uplifting around corners is simulated.

The brick element (CHX60 in DIANA) is a twenty-node isoparametric solid element. It is based on quadratic interpolation and Gauss integration. The interface element (CQ48I in DIANA) is the element between two planes (8 + 8 nodes) in three-dimensional configuration. The element is based on quadratic interpolation. Truss element for reinforcement contains 2 nodes. Figure 22 shows the meshing and element type of materials respectively.

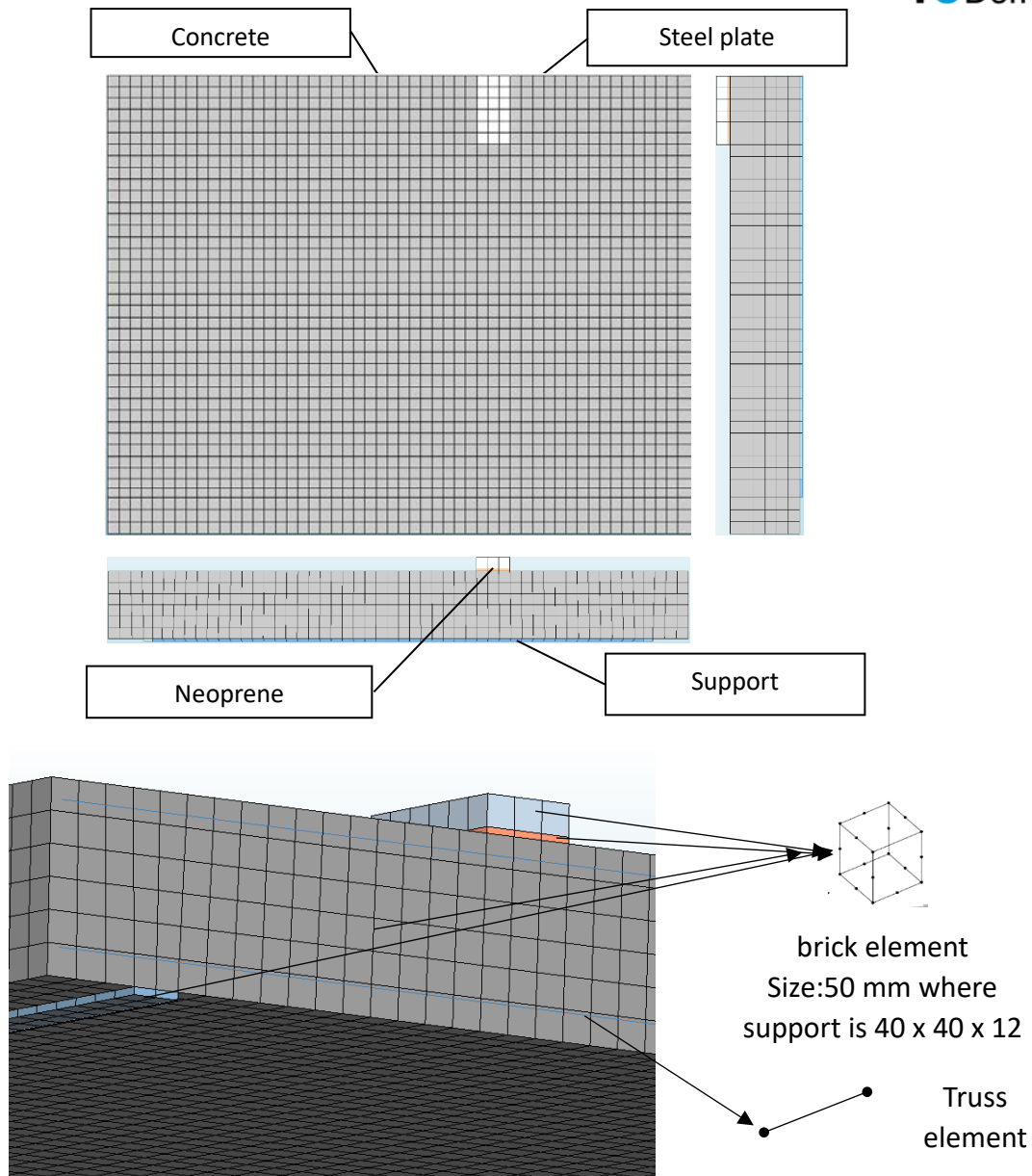


Figure 22 Finite element mesh

The concrete compressive strength corresponding to the mixture used for the specimens was identified from the cylinder compression tests measured on the day the slabs were tested. The modulus of elasticity and the tensile strength were also experimentally obtained with a splitting test. These inputs are chosen from experiments. Other parameters are calculated following the Dutch Guideline (Hendriks *et al.*, 2017) shown in Table 7. Note that the calculation of G_c refers to the MC 1990 that $G_c = 100G_f$, which is also used in Nana *et al.* (2017). Inputs for slab without uniaxial in-plane load (S2) are summarized in Table 6.

Table 6 Parameters for concrete

Slabs	$f_{cm,cyl}$ [MPa]	$f_{ctm,cyl}$ [MPa]	Young's modulus [GPa]	G_F [Nmm/mm ²]	G_c [Nmm/mm ²]
S2	30.9	2.9	31.75	0.135	13.5

Table 7 Parameter calculation: a) concrete; b) steel. (Chapter 2.3.2, Hendriks *et al.*, 2017)

Parameter (Model Code 2010)	
Characteristic cylinder compressive strength	f_{ck}
Mean compressive strength	$f_{cm} = f_{ck} + \Delta f$
Design compressive strength	$f_{cd} = \alpha_{cc} \frac{f_{ck}}{\gamma_c}$
Minimum reduction factor of compressive strength due to lateral cracking	$\beta_{\sigma}^{\min} = 0.4; \beta \geq \beta_{\sigma}^{\min}$ (40% of the strength remains)
Lower-bound characteristic tensile strength	$f_{ctk,\min} = 0.7 f_{ctm}$
Mean tensile strength (for $\leq C50$)	$f_{ctm} = 0.3 f_{ck}^{2/3}$
Design tensile strength	$f_{ctd} = \frac{f_{ctk,\min}}{\gamma_c}$
Fracture energy	$G_F = 73 f_{cm}^{0.18}$
Compressive fracture energy, (Nakamura and Higai, 2001)	$G_C = 250 G_F$
Young's modulus after 28 days	$E_{ci} = E_{c0} \left(\frac{f_{cm}}{10} \right)^{1/3}$
(Initial) Poisson ratio	$\nu = 0.15$
Density plain concrete	$\rho = 2400 \text{ kg/m}^3$
Density reinforced concrete	$\rho = 2500 \text{ kg/m}^3$
Concrete safety coefficient	$\gamma_c = 1.5$
Long term effect coefficient	$0.8 < \alpha_{cc} < 1$

(a)

Parameter	
Characteristic yielding strength	f_{yk}
Characteristic ultimate strength	f_{tk}
Mean yielding strength	$f_{ym} \geq f_{yk} + 10$
Design yielding strength	$f_{yd} = \frac{f_{yk}}{\gamma_s}$
Design ultimate strength	$f_{td} = \frac{f_{tk}}{\gamma_s}$
Class A: $(f_u/f_y)_k \geq 1.05$	$\epsilon_{uk} \geq 2.5\%$
Class B: $(f_u/f_y)_k \geq 1.08$	$\epsilon_{uk} \geq 5\%$
Class C: $\leq 1.15 (f_u/f_y)_k \leq 1.35$	$\epsilon_{uk} \geq 7\%$
Class D: $\leq 1.25 (f_u/f_y)_k \leq 1.45$	$\epsilon_{uk} \geq 8\%$
Design ultimate strain	$\epsilon_{ud} = 0.9 \epsilon_{uk}$
Poisson ratio	$\nu = 0.3$
Density steel	$\rho = 7850 \text{ kg/m}^3$
Steel safety coefficient	$\gamma_s = 1.15$

(b)

3.4.2 Boundary conditions

The support system is simulated as a layer of steel plate supported by a line support. A line is positioned at the middle of steel plate and imprinted in the steel. As a simply supported system, only vertical direction is restrained. The continuous line support is shown below. In this figure, four divided steel support plates can be seen. This refers to the modelling of Nana *et al.* (2017). The reason is that when four plates are separated, better shape of mesh can be generated.

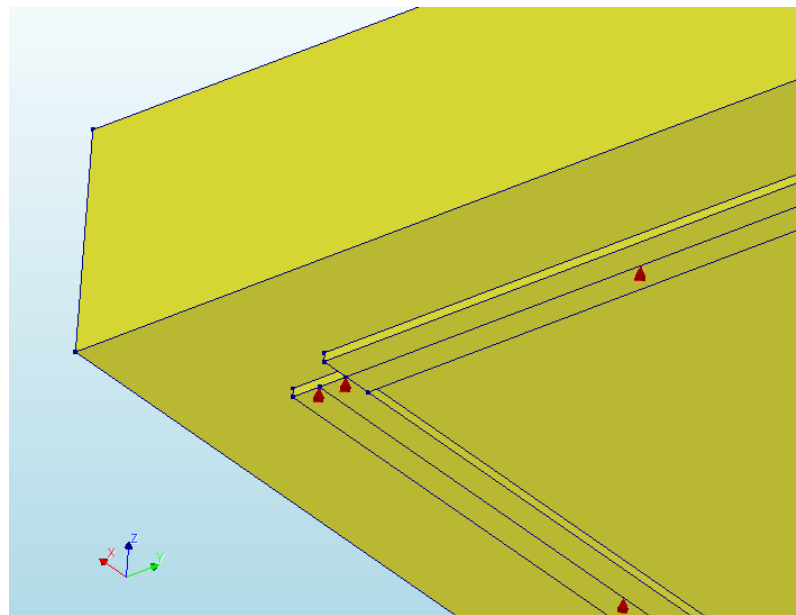


Figure 23 Support system

To reduce the calculation cost, only half of the slab is modelled due to the slab is symmetric. The symmetrical surface is restrained about deformation in Y-direction, which can be seen in Figure 24.

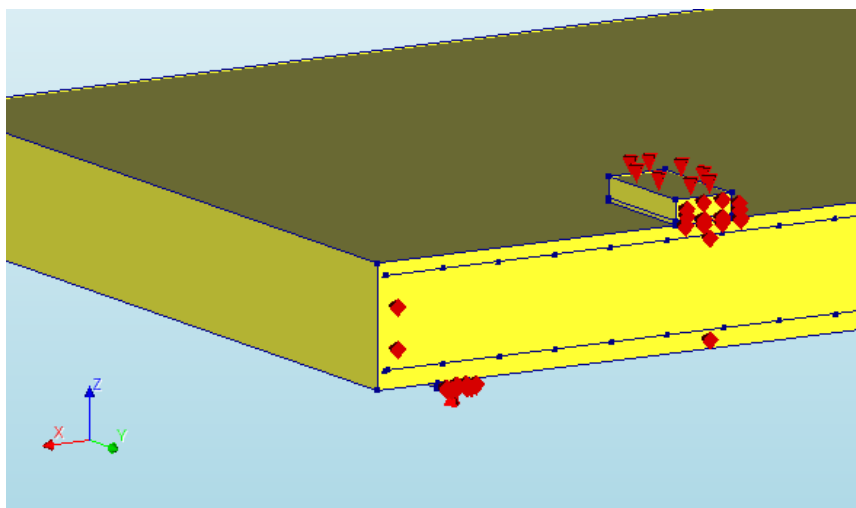


Figure 24 Boundary conditions in symmetrical surface and loading support

3.4.3 Loading method

The out-of-plane load in vertical direction is a distributed load on the top of loading plate. Displacement control is applied to model this load. It is found that the displacement control can result in a better convergence and the final shear load – displacement curve is as expected. Thus, this vertical load is simulated as a prescribed displacement as is shown in Figure 25. Then, the vertical support is applied as shown in Figure 25.

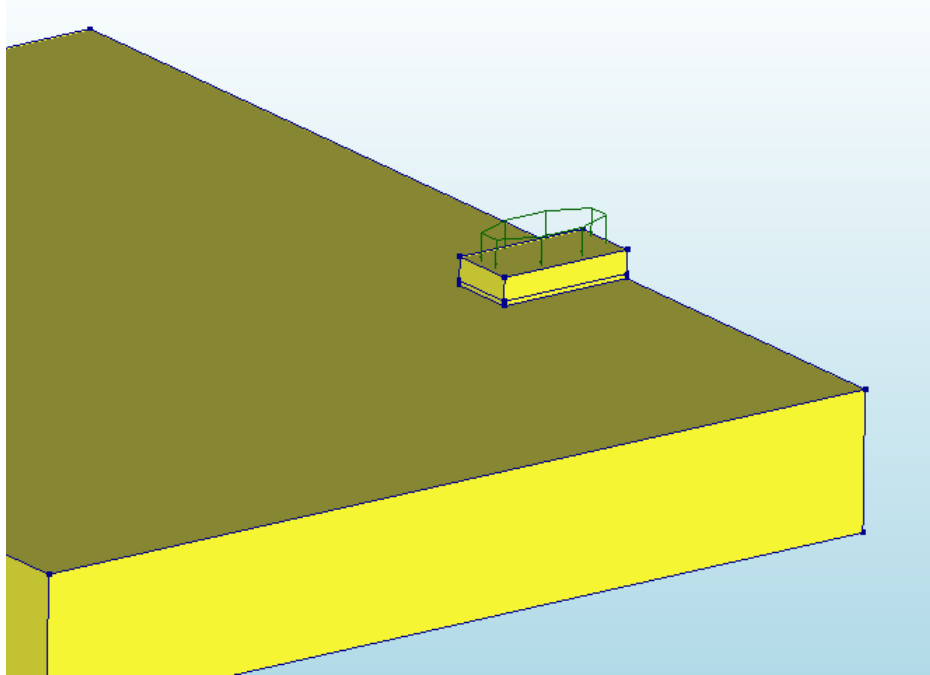


Figure 25 Modelling of out-of-plane force

3.4.4 Analysis method

Newton-Raphson method is applied for each increment, however, when the failure or cracks occur, there is not always convergence. The convergence criteria are force norm with 0.001 tolerance; and energy norm with tolerance 0.001. The maximum iteration is 50 each increment. The modelling choice can be summarized in the Table 8.

Table 8 Modelling choices

Modelling of material		
Concrete	Mass density	2.5 [T/mm ³]
Finite elements		
Element type	CHX60	20-node solid brick element
Element size	50 [mm]	
Material properties		
Material model	Total strain-based crack model	fixed
Crack bandwidth	50 [mm]	
Linear properties	Young's modulus	From Table 6 and 15
	Poisson's ratio	0.15
	Tensile curve	Exponential
Tensile behaviour	Tensile strength	From Table 6 and 15
	Tensile fracture energy	$G_F = 0.073 f_{cm}^{0.18}$
	Poisson's ratio reduction	Damage based
	Compression curve	Parabolic
Compressive behaviour	Compressive strength	From Table 6 and 15
	Compressive fracture energy	$G_C = 100G_F$
	Reduction model	Vecchio & Collins 1993
	Lower bound reduction curve	0.4
	Stress confinement model	no increase
Shear behaviour	Shear retention function	Damage based
Steel (plate)	Mass density	0.0617 [T/mm ³]
Finite elements		
Element type	CHX60	20-node solid brick element
Element size	50 [mm]	
Material properties		
Material model	Linear elastic isotropic	
Linear properties	Young's modulus	210000 [MPa]
	Poisson's ratio	0.3
Reinforcement		
Reinforcement	Mass density	0.0617 [T/mm ³]
Finite elements		
Element type	Truss element	
Material properties		
Material model	Embedded	
Linear properties	Young's modulus	210000 [MPa]
	Plastic hardening	No hardening
Von Mises plasticity	Yield stress	500 [MPa]

Neoprene	Mass density	1.6 [T/mm ³]
Finite elements		
Element type	CHX60	20-node solid brick element
Element size	50 [mm]	
Material properties		
Material model	Rubber solid element	
Linear properties	Young's modulus	7.8 [N/mm ²]
	Poisson's ratio	0.47
Interface (between concrete and supporting steel plate)		
Finite elements		
Element type	CQ48I	"8+8"-node 3D interface element
Element size	50 [mm]	
Material properties		
Material model	Linear elastic 3D surface interface	
Linear properties	Normal stiffness modulus-z	30000 [N/mm ³]
	Shear stiffness modulus-x	30000 [N/mm ³]
	Shear stiffness modulus-y	30000 [N/mm ³]
Discrete cracking	Tensile strength	1e-05 [N/mm ²]
	Mode-I tension softening criterion	Brittle
	Mode-II shear criterion for cracking development	Zero shear traction
Loading, Iteration and Convergence Criterion		
Loading	Out-of-plane	Displacement control
Increment steps	Out-of-plane	0.01 (80)
Equilibrium Iteration	Regular Newton Raphson	
Maximum Number of Iterations	50	
Force norm	tolerance	0.001
Energy norm	tolerance	0.001

3.5 Alternative modelling

According to the numerical modelling from Nana *et al.* (2017), structural behaviour from nonlinear finite element analysis is stiffer than the experiment. The same situation is observed in this thesis study. Thus, some alternative studies are taken by NLFEA by changing modelling choices that are considered as influential factors. In this chapter, the method of these alternative NLFEA will be introduced. Alternative nonlinear finite element analysis is only applied on the slab without uniaxial loads (S2).

3.5.1 Tensile fracture energy (Gf)

The fracture energy of concrete G_f is defined as the energy required to propagate a tensile crack of unit area. When applying the concrete nonlinear exponential tensile curve, the fracture energy is shown in the Figure 26.

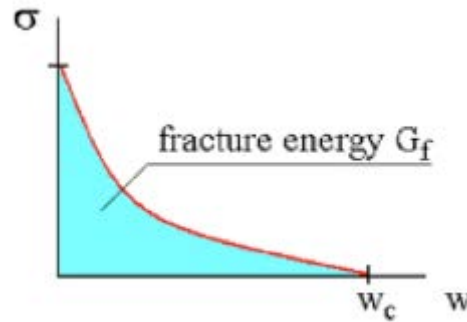


Figure 26 Nonlinear exponential softening curve

To keep the concrete tensile strength constant, fracture energy might be influential to the stiffness of NLEFA slab. From previous study, fracture energy is sensitive and small change will cause big difference for concrete structural behaviour. Thus, 90% and 80% fracture energy are used. And the results comparison is made mainly about S2 to study the influence of fracture energy on the structural stiffness behaviour. Note that the change of fracture energy will keep the tensile strength constant, then according to Figure 26 the displacement will be smaller to reduce the fracture energy.

3.5.2 Total strain-based crack model with Rotating crack

In previous numerical modelling, total strain-based crack model with fixed crack is used. This means that during the loading, once the crack occurs, its direction will not change. In smeared cracking model, cracks are located within the element and behave as a straight line. However, this differs from the reality. This may lead to inaccurate results especially when elements are coarse.

When rotating crack model is applied, direction of cracks can change during loading process, which can simulate the reality more accurate. Thus, numerical results with lower stiffness is expected.

3.5.3 Bond-slip reinforcement

When applying embedded reinforcement, fully – bonded relation between steel bars and concrete is used. And slip between reinforcement and concrete will not happen. However, slip may occur in experiment when the maximum bond stress is reached. TNO Diana offers the bond – slip reinforcement model to precisely simulate the reinforced concrete slab.

The reinforced slab in this study contains reinforcement in both longitudinal and transverse direction with similar reinforcement ratio. The difference between fully – bonded reinforcement and bond – slip reinforcement could have strong influence on the stiffness of slab. Bond-slip reinforcement properties are set as Table 9.

Table 9 Bond – slip reinforcement properties

Reinforcement	Mass density	0.0617 [T/mm ³]
Finite element		
Element type	Truss element	
Material properties		
Model	Bond – slip reinforcement	
Linear properties	Young's modulus	200000 [N/mm ²]
	Plasticity model	No plasticity
Bond – slip interface	Normal stiffness modulus	200000 [N/mm ³]
	Shear stiffness modulus	80769 [N/mm ³]
	Shima bond – slip function	
Bond – slip interface failure model	Compressive strength	From Table 6 and 15
	Diameter per bar	From Table 6 and 15
	Factor to shear – stress	1

3.5.4 Modelling of mortar layer

According to Nana *et al.* (2017), the stiffer structural behaviour in numerical modelling is due to the lack of mortar layer between concrete and support steel plates. To investigate the influence of mortar layer on the structural behaviour, two methods are applied to simulate mortar layer in NLFEA.

Firstly, the mortar layer has the thickness of 4 mm, which is relatively small compared with element size. Thus, 3D interface is applied. Nonlinear elasticity is applied to simulate the mortar behaviour in compression and tension. When mortar is in compression, the stiffness is set the same as concrete. When it is in tension, extremely small tensile strength is set to model the uplift of slab's corners. The properties of the interface are summarized in Table 10.

Table 10 Mortar 3D interface properties

Mortar		
Finite element		
Element type	CQ48I	"8+8"-node 3D interface element
Element size	50 [mm]	
Material properties		
Model	Nonlinear elastic 3D surface interface	
Linear properties	Normal stiffness modulus-z	7937.5 [N/mm ³]
	Shear stiffness modulus-x	3451.1 [N/mm ³]
	Shear stiffness modulus-y	3451.1 [N/mm ³]
Nonlinear elasticity (Diagram)	Normal stiffness modulus-z	[-10, -79375, 0, 0, 10, 1e-06]
	Shear stiffness modulus-x	[-10, -34510, 10, 34510]
	Shear stiffness modulus-y	[-10, -34510, 10, 34510]

3.6 Results of modelling

3.6.1 Shear load – displacement figure

In Bui *et al.* (2017), the shear load in the figure is calculated according to Navier solution obtained for a simply supported rectangular plate with linear displacement hypothesis (Limam *et al.*, 2017). However, the shear load calculation from ultimate load in this master thesis is not performed once again. The shear capacity in figures below is derived from ultimate load obtained from NLFEA directly and divided by factor 1.63. The factor 1.63 is the value equals ultimate load (P_u) over shear load (V_{exp}) in Bui *et al.* (2017). The displacement is monitored at the location of L5 that is indicated in Figure 1. The shear load – displacement results from modelling of slab without uniaxial in-plane load is shown below together with the experimental result and the result from Nana *et al.* (2017).

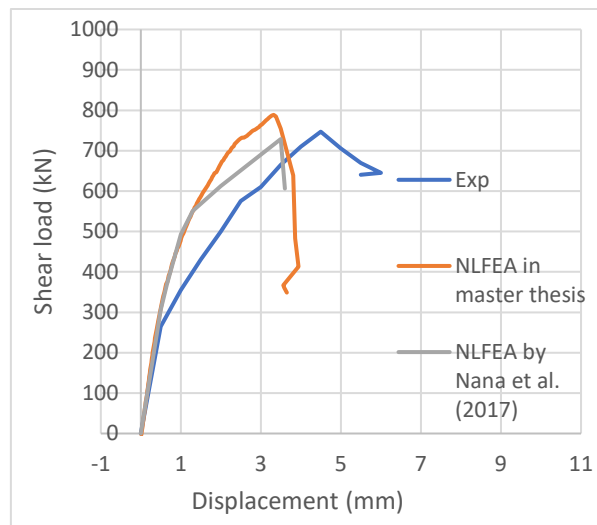


Figure 27 Shear – displacement figures of slab S2

From this figure, it can be found that S2 in numerical model is stiffer when compared to experiments. This stiffer behaviour is found in the NLFEA result from Nana *et al.* (2017) as well.

3.6.2 Development of cracks demonstrated by S2

The development of cracks is described in Bui *et al.* (2017) based on the behaviour of S2. Four critical points are described in chapter 3.1. These four critical points are observed by the curvature change of shear load – strain relation. The similar situation is found in numerical modelling by checking the shear load – strain curve which is shown in Figure 34. Four critical points are observed by the reinforcement strain in experiment, and similar results of first crack (indicated by J1) and transverse crack (indicated by J2 and J4) can be found in NLFEA but not the diagonal tension cracking. Critical points from the experimental results are summarized in Table 11. And critical points are highlighted in the shear load – displacement figure of S2 from both numerical modelling and experiment.

Table 11 Critical points in crack development from experiment

Location	Shear loading [kN]	Description
J1	125	The first crack occurs under the loading plate and due to the bending
J2 and J4	290	Crack in transverse direction occurs
J12 and J13	461	Diagonal tension cracking developed from the loading plate
	747	Ultimate load

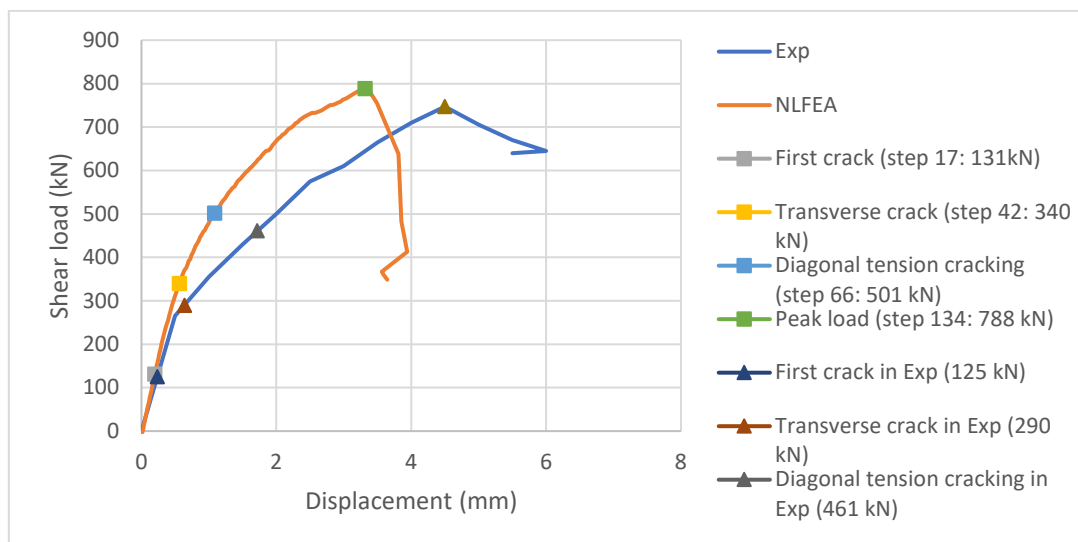
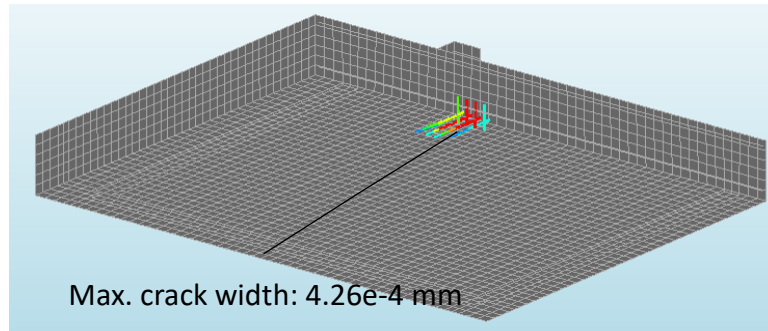
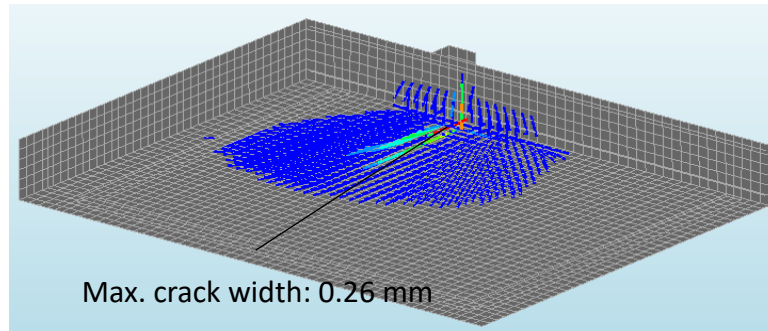


Figure 28 Critical points highlighted in shear – displacement figure both from numerical modelling and experiment (Rectangular points for NLFEA triangular points for experiment)

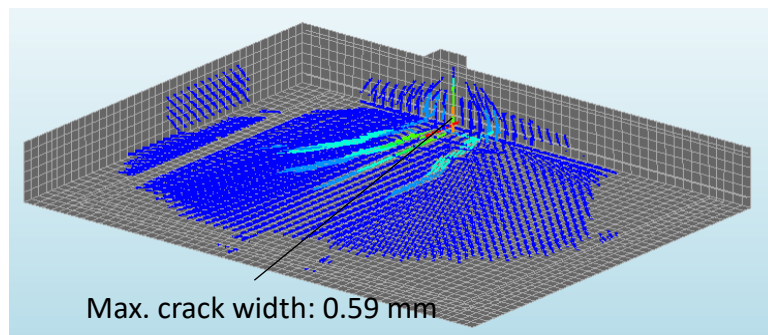
In the numerical modelling, these four critical points are demonstrated by the crack strain figures below. The maximum crack width is indicated in each figure. This process in numerical modelling is similar to the description in experiment. To begin with, at shear loading about 131 kN the first crack is observed. This initial crack occurs under the loading plate and due to the bending. This is monitored by the reinforcement strain at the location of J1. Then, the crack in transverse direction is detected by monitoring the reinforcement strain at J2 and J4 at about 340 kN. When the shear load reaches 501 kN, the big deformation near the support is detected by monitoring the reinforcement strain at J12 and J13. This deformation is due to the development of diagonal cracks from loading plate to the supporting plate. With the increment of vertical load, the diagonal crack width is getting larger. At the ultimate shear load 788 kN, the diagonal crack causes the failure of structure.



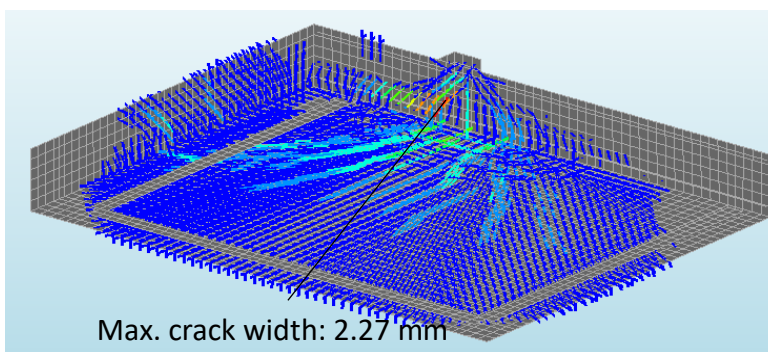
First crack (step 17: 131kN)



Transverse crack (step 42: 340kN)



Diagonal tension cracking (step 66: 501kN)



Peak load (step 134: 788kN)

Figure 29 Crack strain in four critical points of crack development

3.6.3 Crack pattern in Modelling

The crack pattern in NLFEA is discussed when structure reaches the failure load. During the loading process, the development of the “cone” that is the signal of punching shear failure mechanism. Failure mechanism of structure in NLFEA indicates that the slab is more likely failed in punching shear while it is demonstrated that the failure of structure in experiment is due to one – way shear. The figure below shows the crack pattern of bottom view. And the model is mirrored along the symmetrical surface to show the whole bottom of slab. Nevertheless, the one-way shear failure crack along the ledge of support steel plate that is observed in experiment is not observed here. Figure 31 show the development of “cone” due to punching shear in four critical points respectively. The crack that causes the failure at the ultimate load is shown in Figure 32.

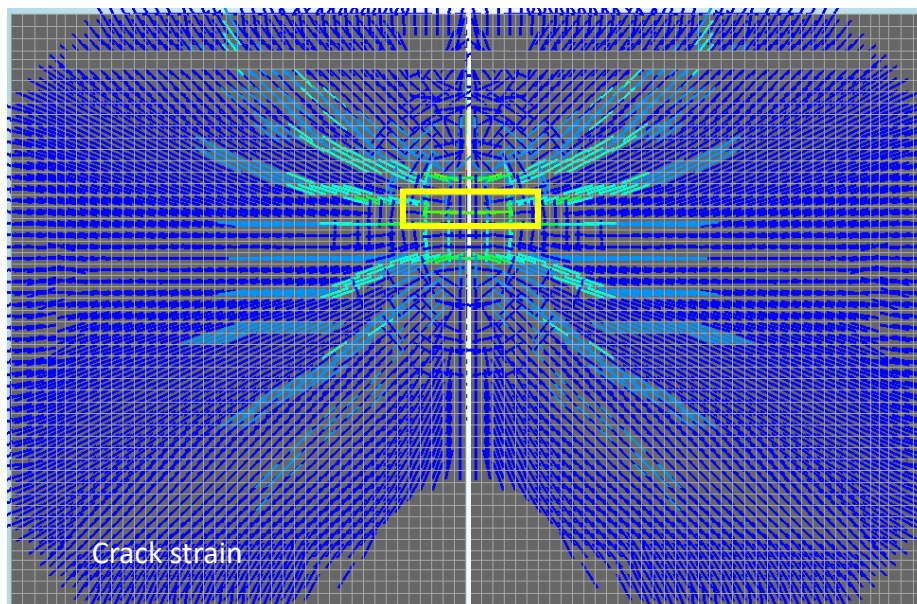
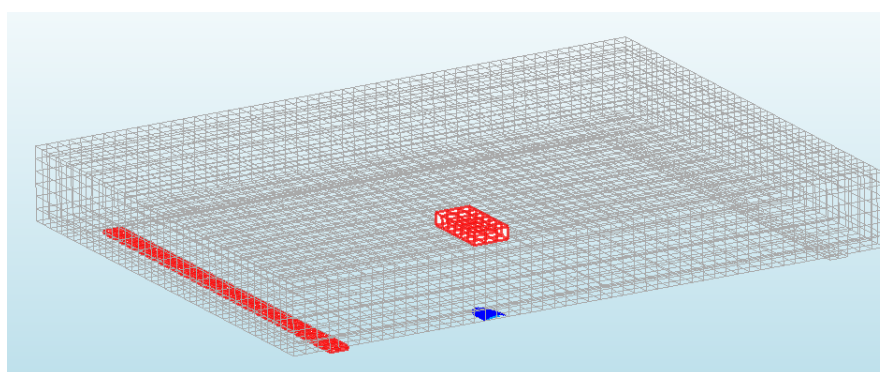
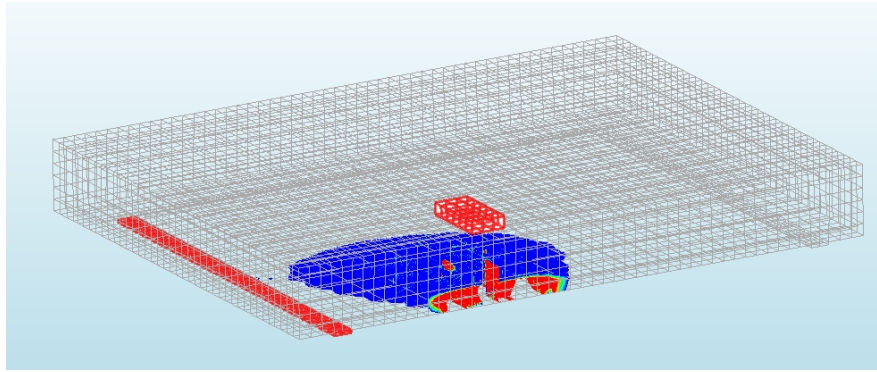


Figure 30 Crack pattern of slab at ultimate load (bottom view)



First crack (step 17: 131kN)

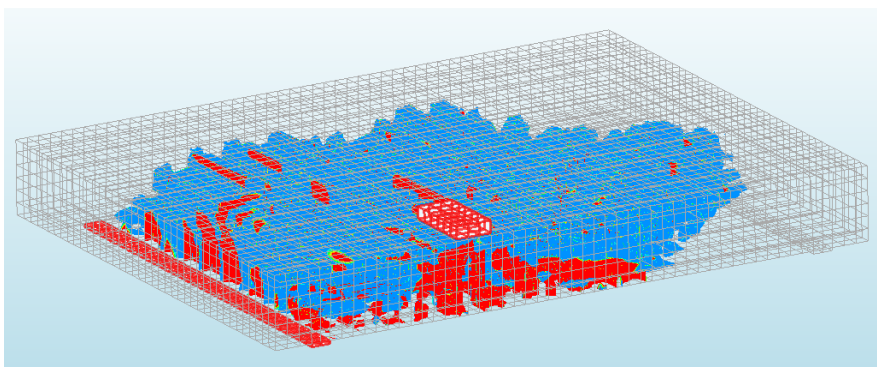
Figure 31 Development of the “cone” by punching shear indicated by crack width



Transverse crack (step 42: 340kN)



Diagonal tension cracking (step 66: 501kN)



Peak load (step 134: 788kN)

Continue of Figure 31

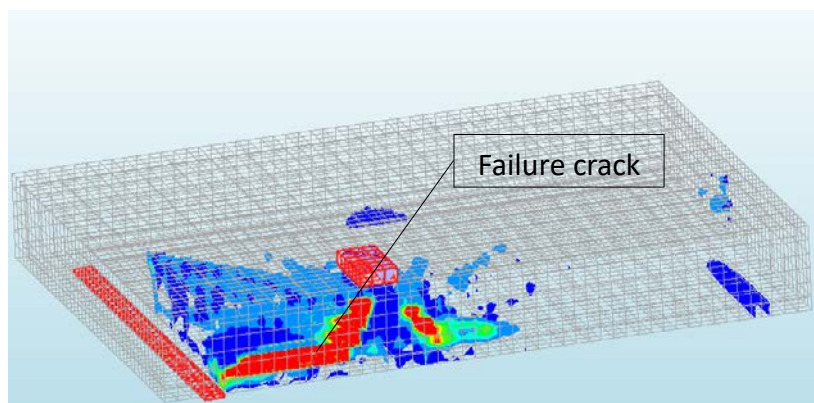


Figure 32 Failure crack under ultimate load

3.6.4 Reinforcement behaviour

Same as the experiment, the cracking following the position of reinforcement layer is observed at the bottom in modelling. At the peak load, using Fe500B reinforcement, no reinforcement yields. The top layer of reinforcement is under compression and bottom layer is in tension. In addition, reinforcements in tension at the bottom at ultimate load can indicate the “cone” under loading plate and prove that the failure mechanism in numerical analysis is more likely punching shear.

Due to the fully-bonded reinforcement, steel bars take part of loads before failure of structure. Then when the ultimate load is reached, cracks fully developed in the punching shear type. At this moment, no yielding of reinforcement is observed. Then along with the increment of vertical load, stress redistribution is observed in reinforcement. Reinforcements located at the big crack position take the load and elongate until the yielding. Figure 34 shows the shear load – strain relation in NLFEA. It can be seen from Figure 34 that reinforcements behave stiffer in NLFEA than those in experiment.

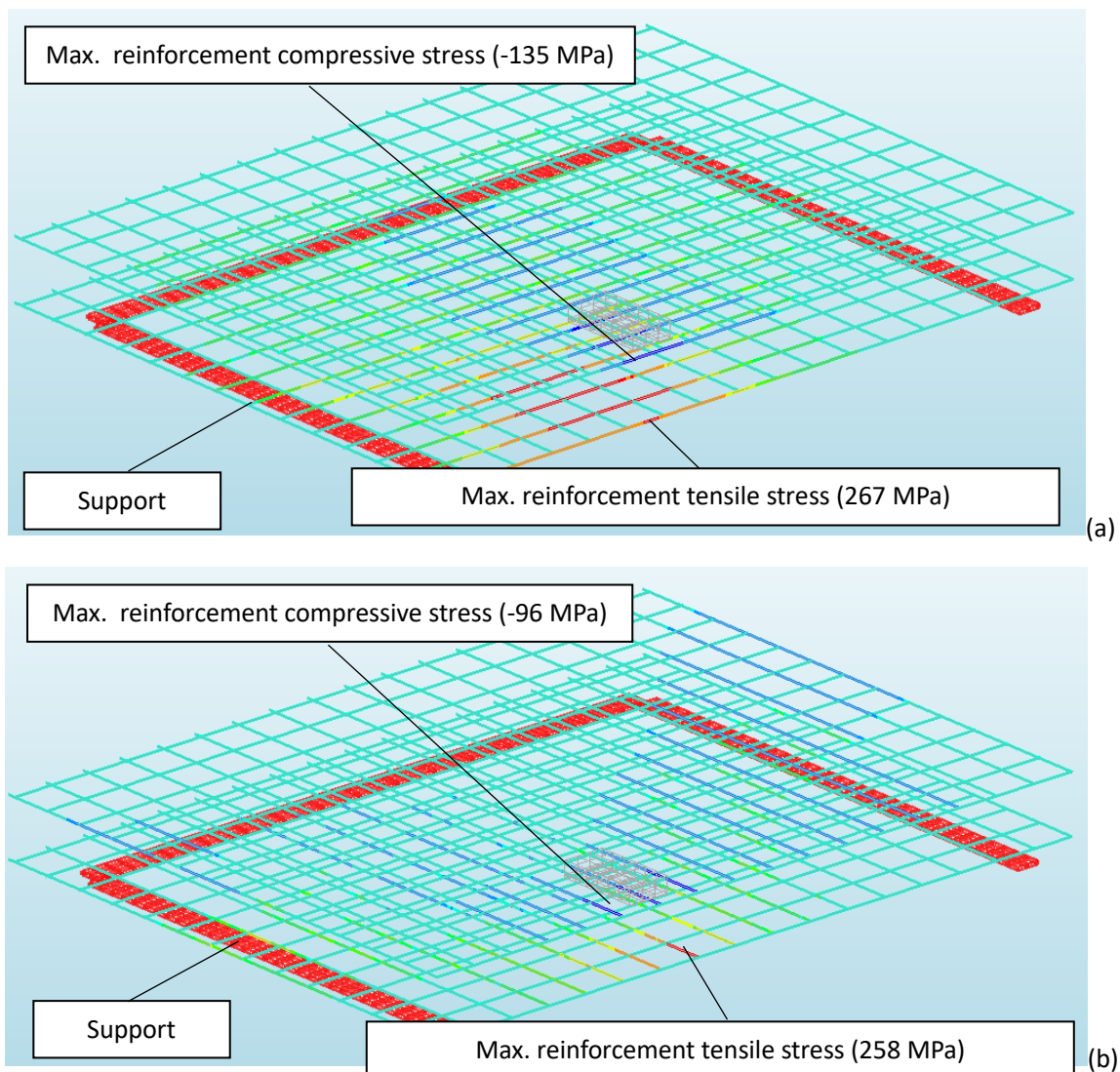


Figure 33 Reinforcement behaviour in NLFEA: a) Longitudinal reinforcement stress; b) Transverse reinforcement stress

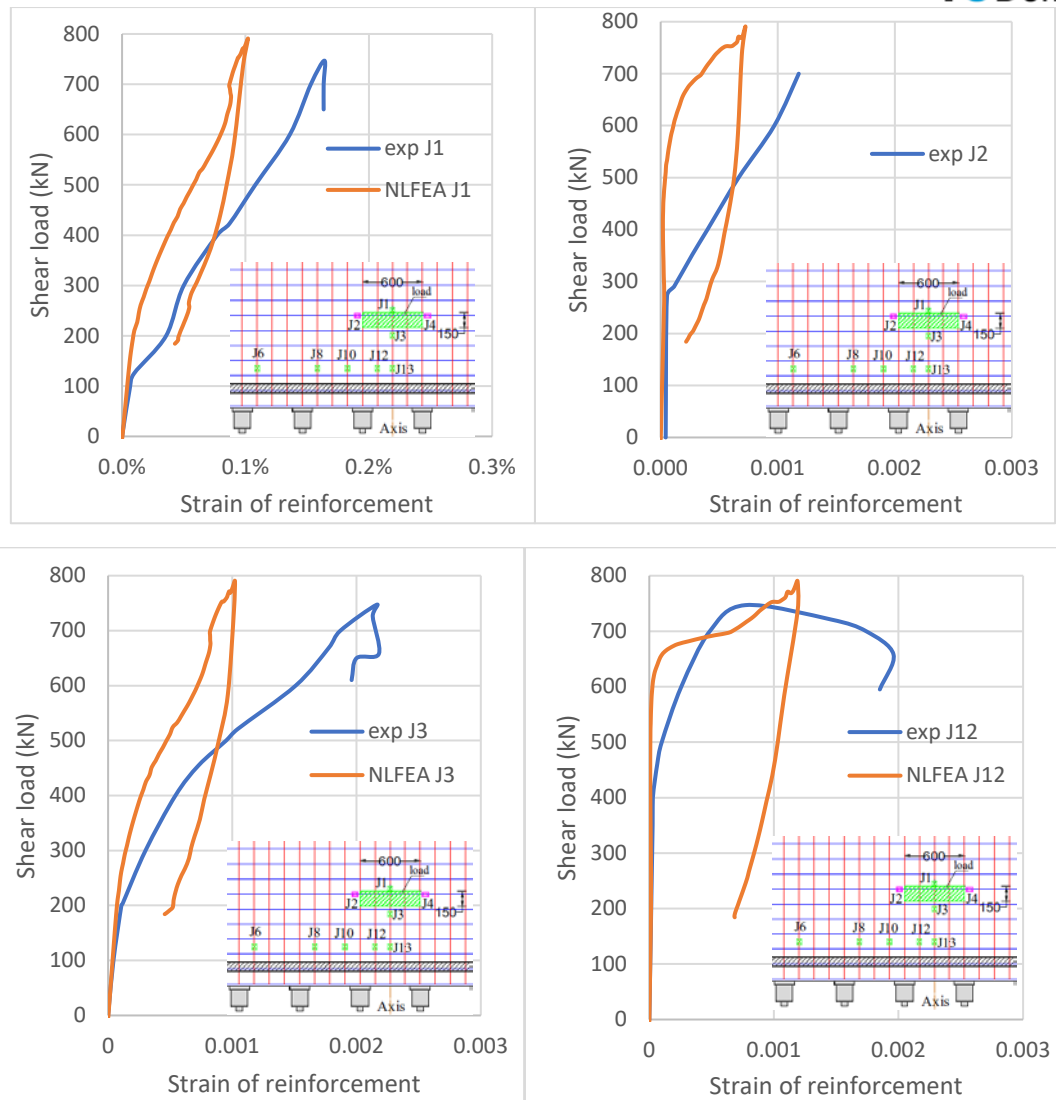


Figure 34 Shear load – strain relation of reinforcement

3.7 Results of alternative modelling

Due to the stiffness of slab in numerical modelling is differ from it in experiment, alternative studies are performed on S2 by changing some influential modelling choices in nonlinear finite element analysis. Although alternative NLFEA has influence on many aspects of structural behavior, the results mainly focus on the stiffness of slabs. Therefore, in this chapter shear load – displacement figure is mainly shown as the result.

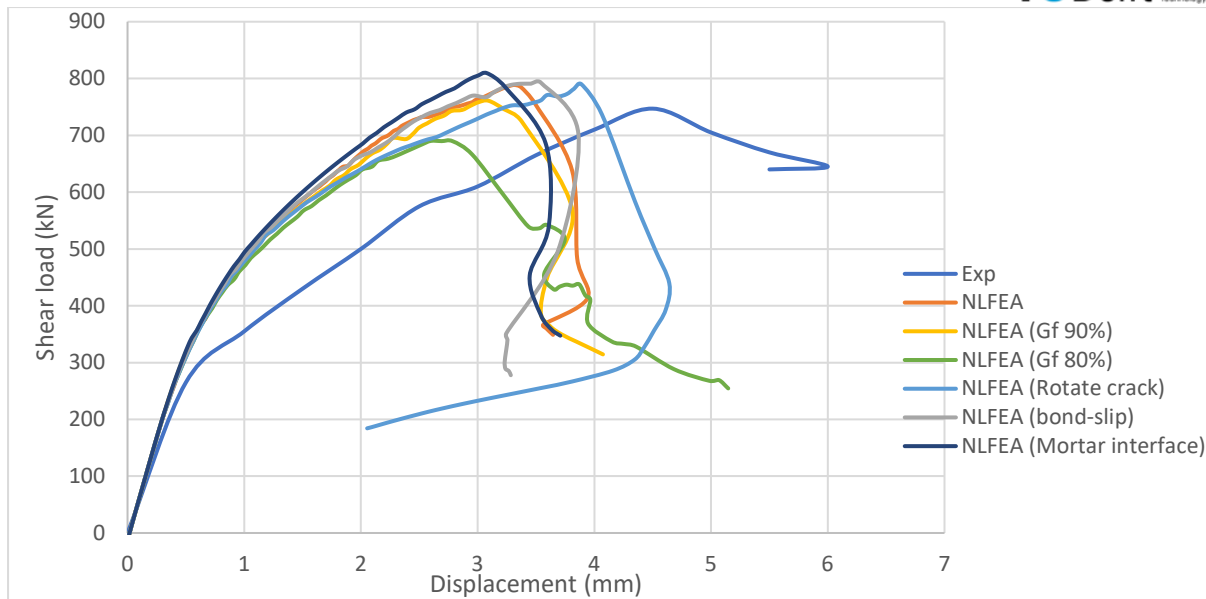


Figure 35 Results of alternative studies on S2

The initial stiffness of slabs in NLFEA is similar to it in experiment. However, changing the variables does not help to simulate the structure more accurate. From Figure 35, all results of NLFEA show stiffer structural behaviour. In Table 12, the comparison among original NLFEA and alternative studies is made.

Table 12 Shear capacity results of alternative studies

Slab No.	NLFEA	Gf 90%	Gf 80%	Rotating crack	Bond-slip reinforcement	Mortar interface
Shear capacity (kN)	788.6	760.9	690.2	771.1	792.2	809.3
Percentage	100%	96%	88%	98%	100%	103%

In addition, the results of these alternative studies have some influence on other aspects of original structure behaviour, for example, the crack pattern is optimized by using rotating crack model rather than fixed crack model. These influences will be introduced and analyzed in next chapter.

3.8 Discussion of results

3.8.1 Crack pattern comparison between NLFEA and experiment

The crack pattern in experiment is described in chapter 3.1 and in NLFEA described in chapter 3.6.1. In this chapter, results are compared and analyzed.

Firstly, it is stated in the experiment that the failure crack is one-way shear crack along the edge of support steel plate. Even the slab is designed to be fail in one-way shear using that

the a_v/d ratio is chosen to be sufficiently large to avoid the direct transmission of the loads to the supports ($a_v/d = 2.1$). In Bui *et al.* (2017), failure crack near support is drawn in the Figure 11. However, the crack is not observed in this NLFEA and the numerical modelling from Nana *et al.* (2017). The comparison of crack pattern from bottom view of slab is summarized in Figure 36.

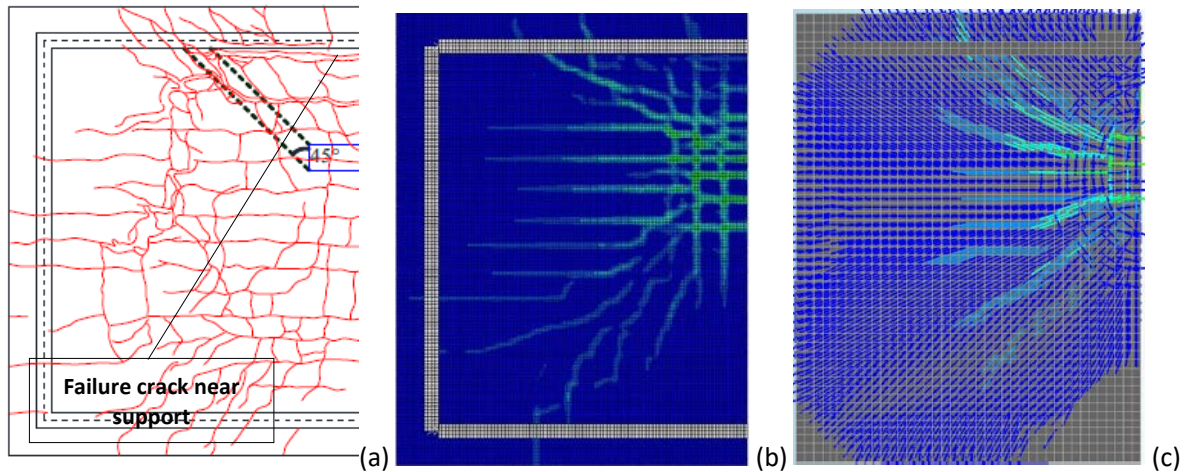


Figure 36 Comparison of crack pattern of bottom view: a) Experiment from Bui *et al.* (2017); b) NLFEA from Nana *et al.* (2017); c) NLFEA from this master thesis

Secondly, when checking the crack pattern from the middle symmetrical surface (Figure 32), the similar cracks can be observed. The design of a_v/d to avoid the transmission of load directly through support is valid both in experiment and NLFEA. In Limam *et al.* (2017), discussion about the failure mode is made. In the experiment, it is stated that the first overload failure is observed near the support, and further post mortem tests, for example saw-cuts, are made to confirm this. Shear capacity calculation is made based on Eurocode 2 for one-way shear by Bui *et al.* (2017). And numerical analysis is made by Nana *et al.* (2017). All these researches confirm the one-way shear is the failure mode. However, the failure crack near support is not observed in this master thesis. From the view of symmetrical surface in this NLFEA, punching shear crack opening develops as a cone and cracks expand to lead to the final failure in NLFEA.

In addition, it can be found that horizontal crack in symmetrical surface is just above the longitudinal reinforcement layer. The punching shear crack is developed. However, the biggest crack is horizontal crack (highlighted in red in figure above) in the peak load stage. From the aspect of crack pattern, further numerical studies with rotating crack model is recommended to model this kind of structure.

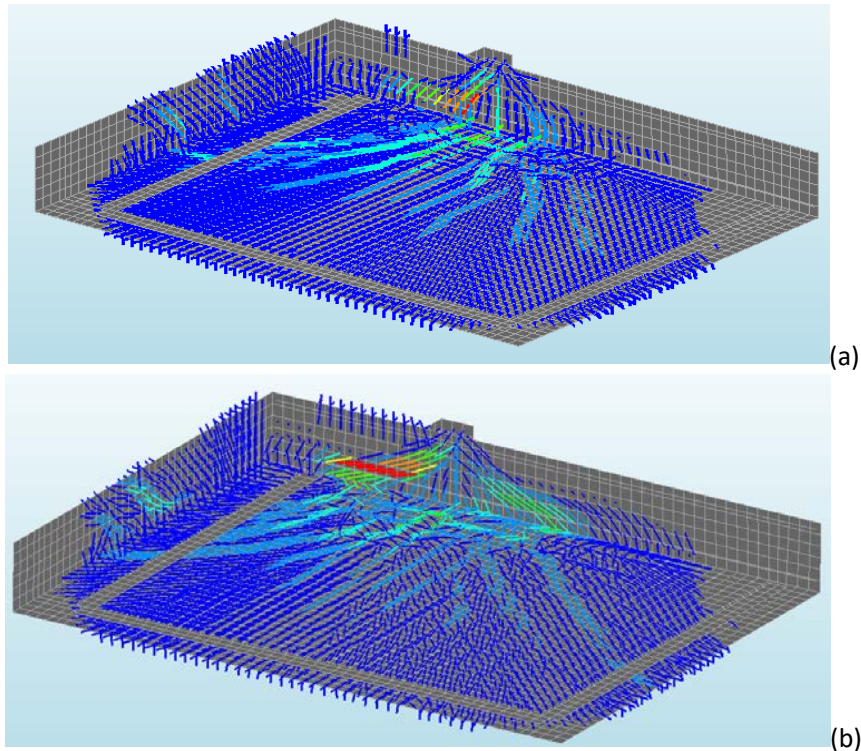


Figure 37 Comparison of crack inclination on S2 at peak load: a) Fixed crack model; b) Rotating crack model

3.8.2 Stiffer slab behaviour in NLFEA

In chapter 4, stiffer behaviour of slab is observed in NLFEA than in experiment. The NLFEA of Nana *et al.* (2017) shows the same results in stiffness aspect. Nana *et al.* (2017) indicates that the absence of mortar layer in modelling between steel supporting plate and concrete could be the reason for this stiffer behaviour. By performing alternative studies, it can be concluded that fracture energy, concrete crack model and modelling mortar are not the main reasons that cause the stiffer behaviour in NLFEA. And it is not sufficient to conclude that bond-slip reinforcement is not the reason although it does not show a softer behaviour in alternative NLFEA.

In the aspect of difference between experiment and modelling, the displacement of supporting frame (round bars under supporting plates and I-beam under round bars indicated in Figure 9) is not taking into account in NLFEA. In NLFEA, the support system is simplified and modelled as indicated in chapter 4.1.2 and 4.2.2. The displacement at the position of L5 is monitored by LVDT that is connected to the I-beams by a steel stick. Although this part of test setup is not indicated in Bui *et al.* (2017) clearly, it can be seen from Figure 10. The displacement of supporting frame could be the reason of the stiffer behaviour in NLFEA. This can be verified by modelling the whole supporting system. But the complexity of model and the time cost of NLFEA would increase.

From Figure 33, it can be found that reinforcements in NLFEA behave stiffer than the experiment after the first crack occurs. The reason could be the perfect bonded reinforcement is used in modelling. However, slip between reinforcement and concrete exists in experiment. Bond-slip reinforcement model is the solution. However, by checking the strain of

reinforcement in the alternative NLFEA with bond-slip reinforcement, the bond-slip model does not show the difference from NLFEA with perfect bond reinforcement. One attempt of NLFEA with bond-slip reinforcement is not sufficient to conclude that the perfect bond reinforcement is not the reason of the stiffer slab behaviour in modelling. More specific research and insight should be done in further study to apply bond-slip reinforcement to the modelling of this kind of slabs.

In Nana *et al.* (2017), 20-mm mesh is generated. In this thesis, modelling cannot create finer mesh (smaller than 50 mm) due to the hardware issue. Finer mesh would result in more accurate results such as crack development, shear capacity and stiffness behaviour. Hence, it is suggested that modelling can be improved by using finer mesh.

Another possible reason is that uncertainties are not taken into account of material and model. The inputs (compressive strength, tensile strength and Young's modulus) of concrete model is taken from the tests in experiment. This introduces the uncertainty into modelling. Safety formats in NLFEA are delivered in MC 2010 and Dutch Guideline (Hendriks *et al.*, 2017) to deal with the uncertainties, namely Global Resistance Factor Method (GRF), Partial Safety Factor Method (PF) and Estimation of Coefficient Of Variation of Resistance Method (ECOV). Further studies are suggested by considering the safety factors following these literatures to reduce the influence of uncertainties in NLFEA.

4. Case study of slabs with uniaxial in-plane load

In this chapter, the case study of slabs with uniaxial in-plane load is described based on the slabs in Bui *et al.* (2017). Some slabs are loaded in uniaxial compression (SC1 and SC2), some are in uniaxial tension (ST1, ST2, ST3 and ST4). The test setup of these slabs is similar to the slab without uniaxial in-plane load (S2) except the in-plane loading system. Hence, the in-plane loading system is introduced in this chapter. In addition, the validation of analytical prediction of shear capacity done by Bui *et al.* (2017) is stated as well. Then, the modelling of these slabs is introduced and results are presented. Discussion is made about two parts: the influence of uniaxial in-plane load, and validation of prediction of analytical assessment and numerical assessment.

4.1 Experiment by Bui *et al.* (2017)

Six RC slabs are tested in the experiment with uniaxial in-plane load. Many aspects of these slabs are similar to the slab without uniaxial in-plane load, such as, geometry, material properties and boundary conditions. The similar aspects are described in chapter 3.1 and will not be repeated in this chapter. The difference is mainly the in-plane loading system. In this chapter, in-plane loading system and experimental results are introduced, as well as the validation of analytical prediction of shear capacity according to existing codes.

4.1.1 Material properties

As is mentioned in chapter 3.1, concrete C20/25 and reinforcement FeE 500B are applied. The compressive strength corresponding to the mixture used for the specimens is identified from the cylinder compression tests measured on the day the slabs are tested. The modulus of elasticity and the tensile strength are experimentally obtained in the testing day. Properties are summarized in Table 13.

Table 13 Slab properties of slabs with uniaxial in-plane load

Slab	Axial load (kN)	Axial stress (MPa)	$f_{cm,cyl}$ (MPa)	$f_{ctm,cyl}$ (MPa)	Young's modulus (GPa)	Specimen age at testing
SC2	-1800	-1.5	33.3	3.6	30.75	73
SC1	-1200	-1.0	35.6	3.8	32.65	62
ST1	600	0.5	34	3.0	34.20	49
ST2	780	0.7	34.7	3.8	34.65	45
ST3	1200	1.0	34.2	3.6	33.85	55
ST4	1440	1.2	34.2	3.5	32.40	59

4.1.2 In-plane loading system

The axial force is transferred to the specimens using six metal squares that are locked to connector anchors per square. The connector anchors are welded with embedded vertical rod in concrete slab. Metal squares on one side are coupled with same squares on the other side of slab, using two in-plane bars 30 mm in diameter when loaded in compression. The square system is free in in-plane rotation. When axial tension is applied, in-plane bars are replaced by the empty 11.5-mm-thick tube to better transmit the loading. The jacks that supply axial load are load-controlled independently and in-plane loading system has no connection with

support system. During the tests, axial compression and tension will be applied first, then concentrated load is applied with a constant velocity until collapse. The uniaxial force on each slab can be found in Table 13. The loading system can be described by the Figure 38.

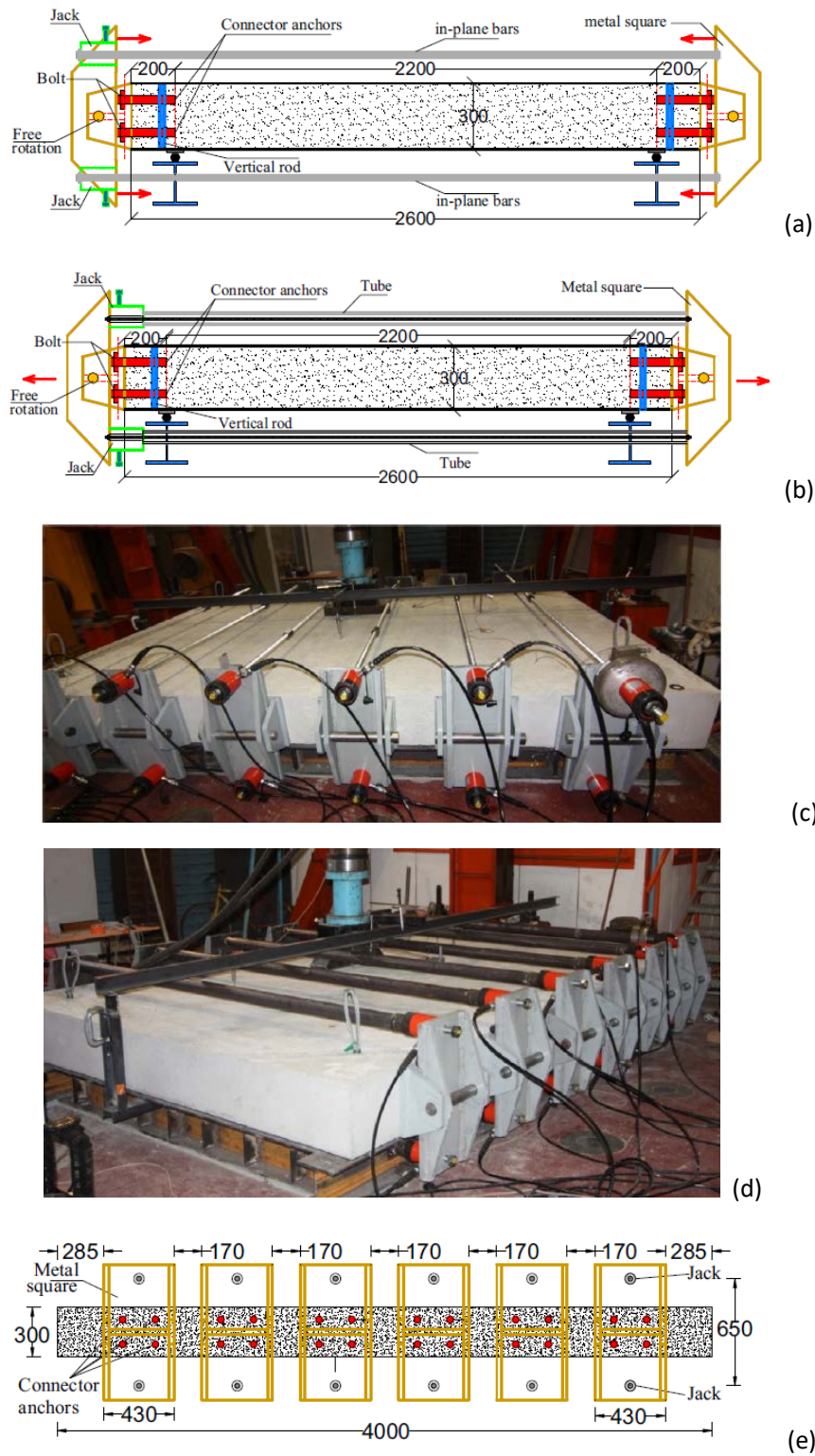


Figure 38 Loading system: a) transverse section of compression; b) transverse section of tension; c) setups of compression; d) setups of tension; e) horizontal section. Units: [mm] (Figure 4, Bui *et al.*, 2017) [mm]

4.1.3 Experimental results

The cracking indication of all slabs are shown in Figure 39.

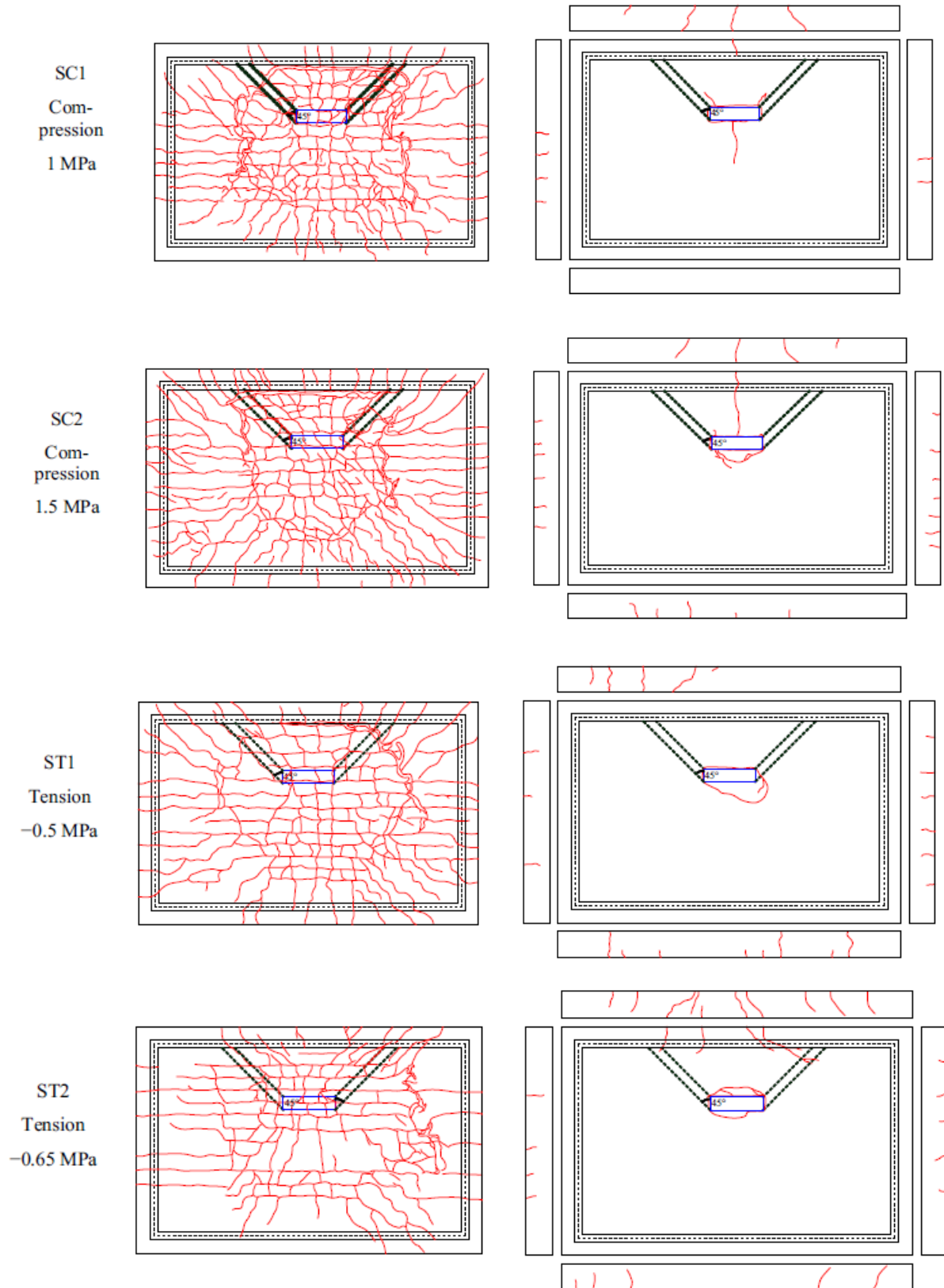
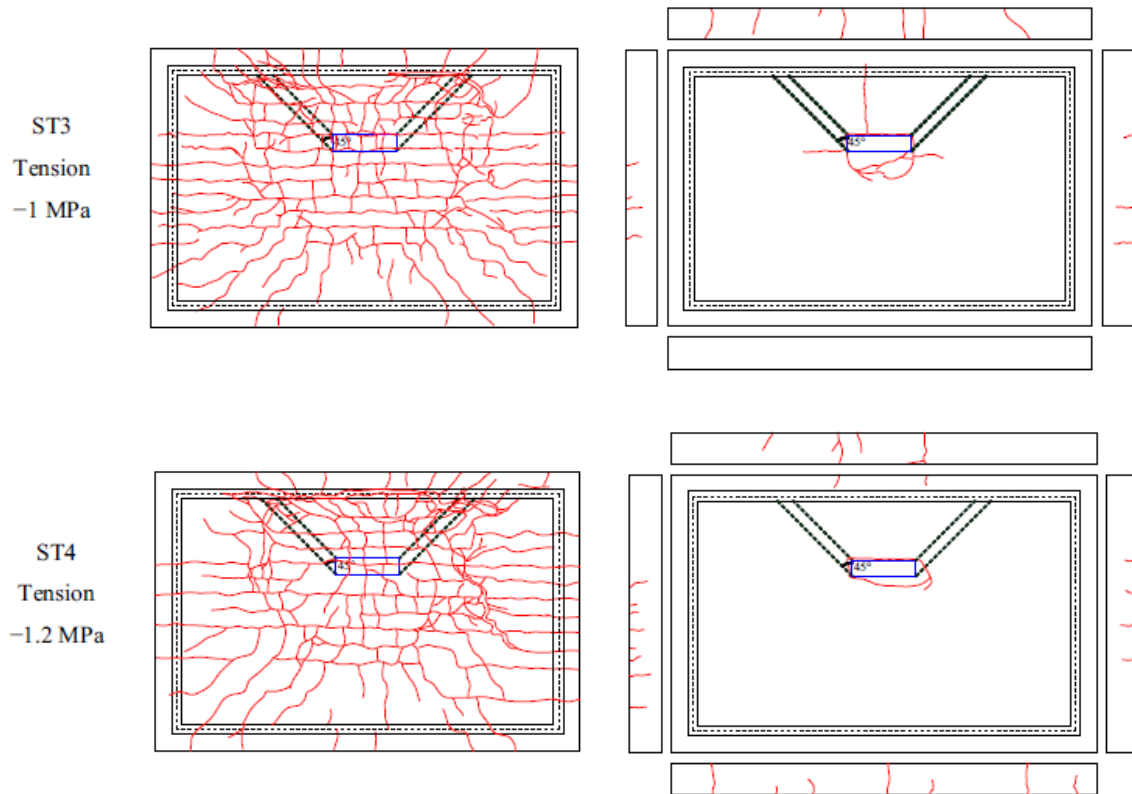


Figure 39 Cracks indication (Figure 7, Bui *et al.*, 2017)



Continue of Figure 39

The shear – displacement figure of these slabs is shown in Figure 40. Note that the figure for slab without uniaxial in-plane load is included as well to show the influence of uniaxial in-plane load on the structural behaviour.

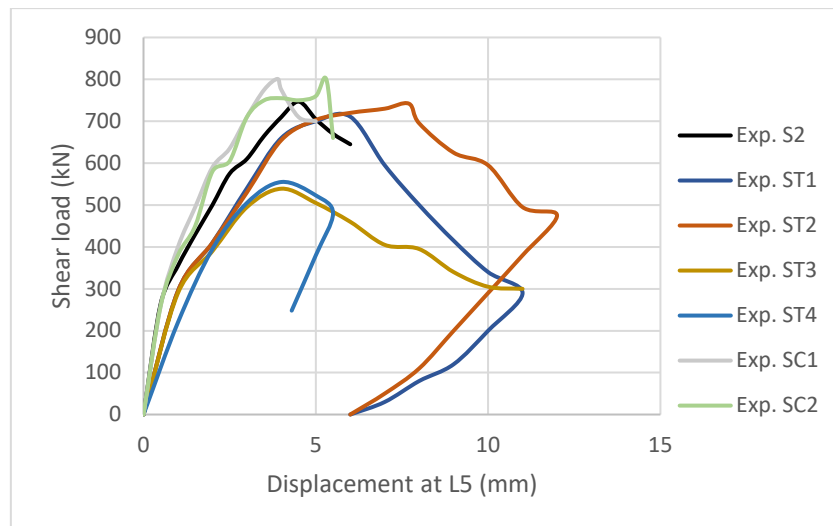


Figure 40 Shear load displacement curve for all slabs

4.1.4 Influence of uniaxial in-plane load

When the uniaxial compression is applied (SC1 and SC2), the same elastic stiffness is obtained as the slab without uniaxial load (S2). In the slab without uniaxial load, the stiffness reduces strongly after around 300 kN of shear load. While the stiffness keeps constant and reduces

slightly later when loaded in uniaxial compression. This is because that the compression can delay the cracking, and higher shear capacity can be found. The sudden drop of the force-displacement curve after post-peak phase can be seen, which means that axial compression causes the brittle failure as well.

The influence of uniaxial compression or tension on the shear strength can be concluded in the Figure 41:

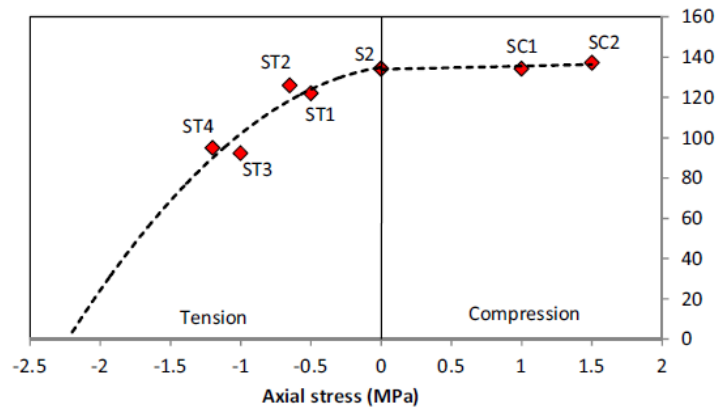


Figure 41 Influence of axial stress on the ultimate shear capacity (Figure 13, Bui *et al.*, 2017)

For slabs loaded in uniaxial tension (ST1, ST2, ST3, ST4), the more tension is applied, the more elastic stiffness reduces when compared with S2. Large ductile behaviour can be observed after post-peak phase as indicated in Figure 40. The shear capacity reduces due to axial tension.

From the Figure 41 it can be concluded that the influence of axial tension on the shear capacity is not linear, and the influence of compression is linear. This may be led by the relative small uniaxial compression stress (1 MPa for SC1 and 1.5 MPa for SC2) compared to the concrete compressive strength (35.6 MPa for SC1 and 33.3 MPa for SC2).

4.1.5 The validation of analytical prediction of shear capacity done by Bui *et al.* (2017)

The validation of analytical assessment of seven slabs is performed in Bui *et al.* (2017) according to Eurocode 2 (EC2), ACI 318-14 and AFCEN ETC-C shear design for nuclear buildings. Note that the shear capacity calculated is combined with two parts: shear strength of slab without uniaxial in-plane force and the shear strength derived from uniaxial in-plane load. The shear strength of slab without uniaxial in-plane force is obtained from experiment (747 kN for S2). The calculation of EC2 is indicated in chapter 2.1.1. The Calculation of ACI 318-14 follows the simplified method when loaded in compression. The calculation of AFCEN ETC-C can be seen in Bui *et al.* (2017) but not reviewed in this thesis. This validation is performed by comparing the shear capacity from experimental results and prediction from design codes. The result is shown in Table 14.

Table 14 Shear strength calculated with predictions of the EC2, ACI 318 - 14 and ETC-C for all slabs

Slab	Axial stress σ_{cp} [Mpa]	$f_{cm,cyl}$ [Mpa]	$V_{total(Experiment)}$ [kN]	V_{EC2} [kN]	$V_{ACI\ 318-14}$ [kN]	V_{ETC-C} [kN]
SC2	1.5	33.3	792	902	835	863
SC1	1.0	35.6	801	886	842	859
S2	0.0	30.9	747	747	747	747
ST1	-0.5	34.0	711	741	704	688
ST2	-0.65	34.7	742	737	687	667
ST3	-1.0	34.2	539	702	626	593
ST4	-1.2	34.2	555	684	594	556

Another set of analytical calculation is made in Bui *et al.* (2017) that the shear strength without the axial load was calculated directly from the formula of the design codes. Collecting previous beam, slab test and slabs tested by Bui *et al.* (2017), the experimental results and analytical predictions are compared. Note that only structures loaded in uniaxial tension are compared here. The conclusion is made that EC2 and ETC-C give unconservative results when slab is subjected to combined shear and tension. While ACI 318-14 should be used for security situation although it is too conservative.

4.2 Modelling of the uniaxial in-plane loading system

The difference between slabs with and without in-plane load is mainly the in-plane load system. Thus, introduction of the modelling in this chapter is focusing on in-plane load system.

4.2.1 Modelling assumption

According to the experiment, in-plane uniaxial load is applied by jacks and transferred by 12 steel plates to concrete slab. All jacks are independent with each other and is load-controlled. The in-plane loading system has no connection to the supporting system. In addition, the in-plane loading plate is free in rotation in the plane. All these experiment setups mean that the in-plane load is constant and stay in horizontal direction during loading process. The Figure 42 indicates this simply. Thus, the mechanical model can simplify in-plane load as distributed load applied on steel plate and is always in horizontal direction.

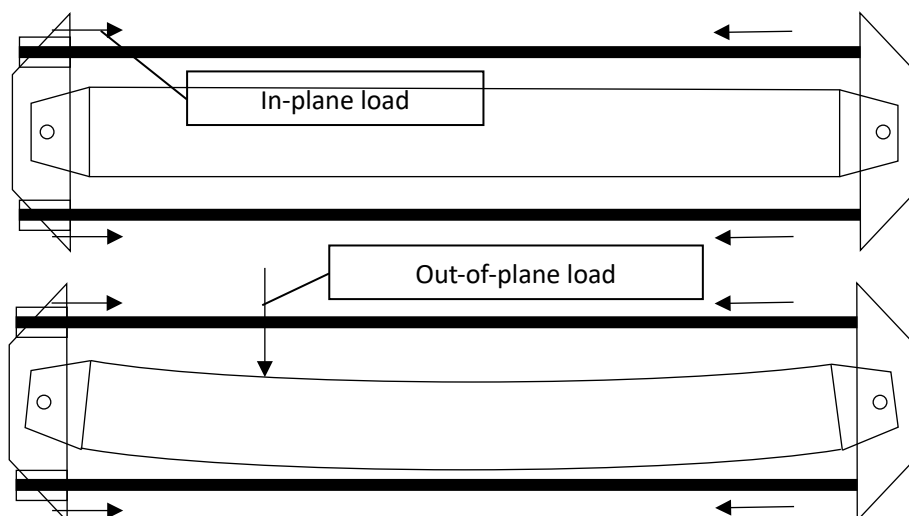


Figure 42 In-plane loading system during loading process (transverse direction not in scale)

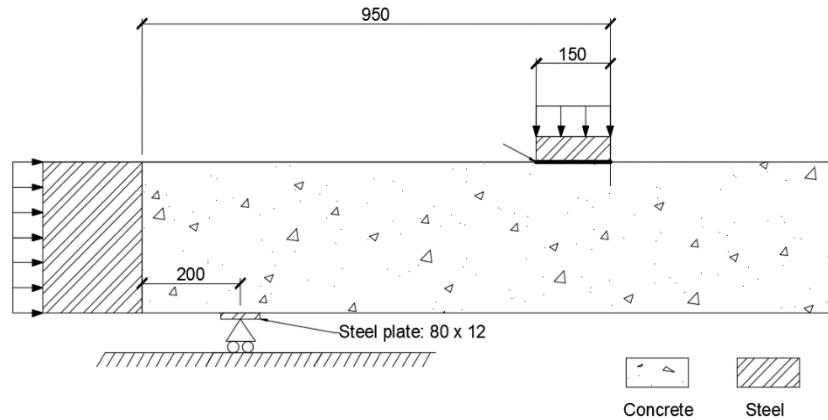


Figure 43 Scheme of in-plane load (transverse direction) [mm]

4.2.2 Modelling choices

Due to the concrete properties are obtained from the tests in experiment, inputs of concrete vary each other. Table 15 contains the inputs used in NLFEA for slabs with uniaxial in-plane load.

Table 15 Various parameters for concrete

Slabs	$f_{cm,cyl}$ [MPa]	$f_{ctm,cyl}$ [MPa]	Young's modulus [GPa]	G_F [Nmm/mm ²]	G_c [Nmm/mm ²]
SC1	33.3	3.6	30.75	0.137	13.7
SC2	35.6	3.8	32.65	0.139	13.9
ST1	34	3	34.2	0.138	13.8
ST2	34.7	3.8	34.65	0.138	13.8
ST3	34.2	3.6	33.85	0.138	13.8
ST4	34.2	3.5	32.4	0.138	13.8

As is explained in chapter 4.2.1, the in-plane uniaxial force can be simplified as Figure 43. Thus, the modelling of in-plane force is the distributed force applied on 12 thick steel plates. The direction of forces is in normal direction then it would not change during loading process. In-plane force is with load control. The thickness of steel plate is 200 mm, relatively thick, to better transfer the in-plane forces to the concrete slab. In addition, self-weight is taken into account. The Figure 44 shows the model of in-plane forces. During the loading increment, in-plane load is force controlled and applied on the structure prior to the out-of-plane load.

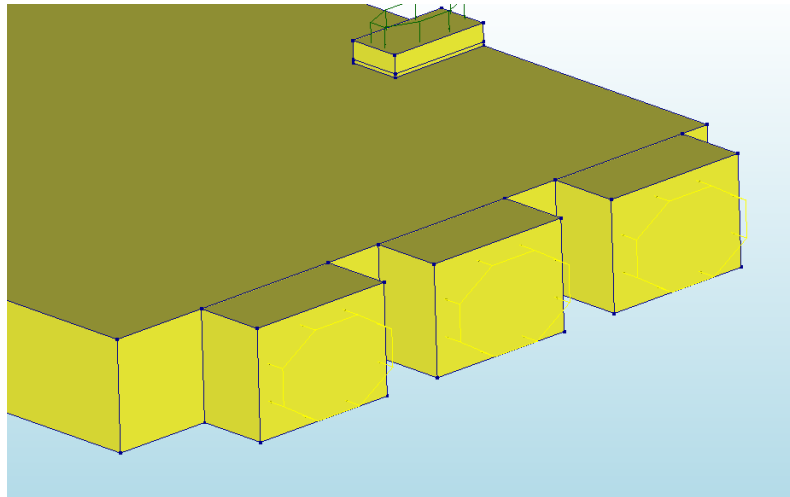
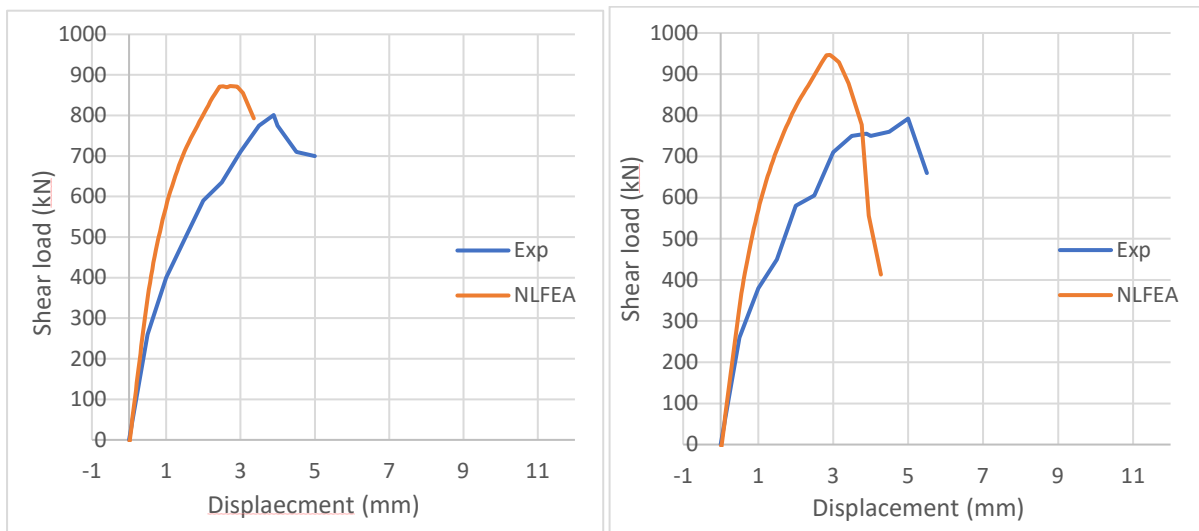


Figure 44 Modelling of in-plane uniaxial force

4.3 Results of modelling

4.3.1 Shear – displacement figure

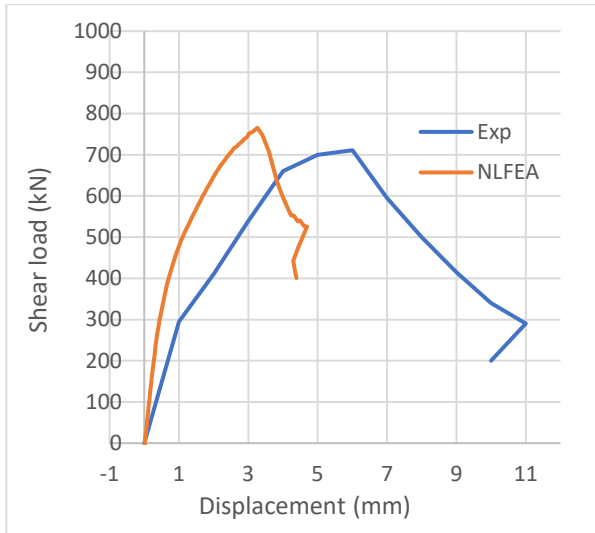
Following the method presented in chapter 3.6.1, the shear load is calculated from ultimate load. The shear load – displacement relation is plotted below together with their experimental figure respectively for six slabs.



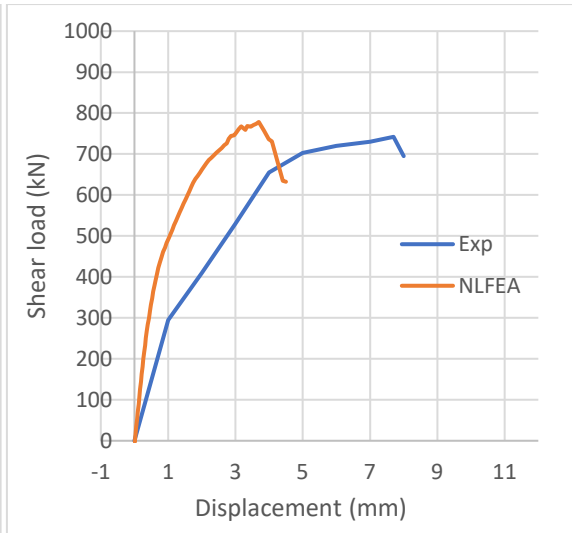
SC1 (uniaxial compression: 1 MPa)

SC2 (uniaxial compression: 1.5 MPa)

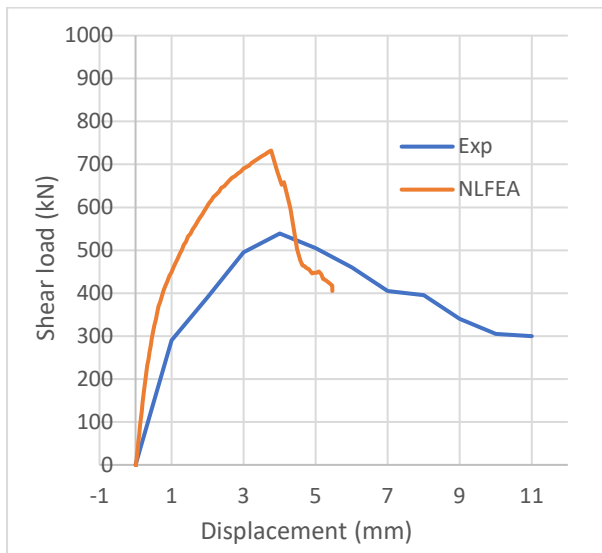
Figure 45 Shear – displacement figures for all slabs with uniaxial in-plane load



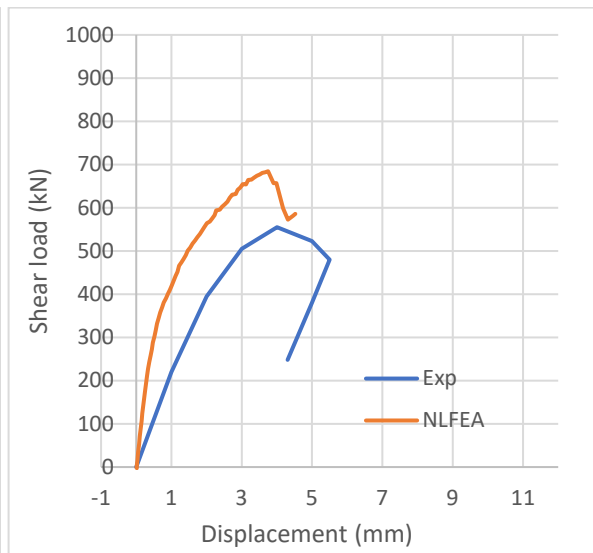
ST1 (uniaxial tension: 0.5 MPa)



ST2 (uniaxial tension: 0.65 MPa)



ST3 (uniaxial tension: 1 MPa)



ST4 (uniaxial tension: 1.2 MPa)

Continue of Figure 45

From this figure, it can be found that all slabs in numerical model are stiffer when compared to experiments. The increase effect of shear load by uniaxial compression in NLFEA is larger than that in experiment. However, the reduction effect of shear capacity by uniaxial tension in NLFEA is smaller than that in experiment. In addition, the brittle behaviour of slabs under uniaxial compression is observed while ductile behaviour for uniaxial tension.

4.3.2 Influence of uniaxial tension and compression

The influence of uniaxial tension and compression on the shear capacity in NLFEA can be summarized in the figure below. In this figure, the rectangular point is the value of uniaxial tension 2.2 MPa, which is the mean tensile strength of C20/25 concrete. The yellow point is another analysis with uniaxial compression 2 MPa to reveal the influence of uniaxial compression on the shear capacity. The vertical axis takes into account the influence of concrete compressive strength because each slab has different concrete compressive strength.

From this figure, it can be concluded that compression increases shear capacity and tension reduces it. Higher the uniaxial compression, higher the shear capacity and the same for uniaxial tension.

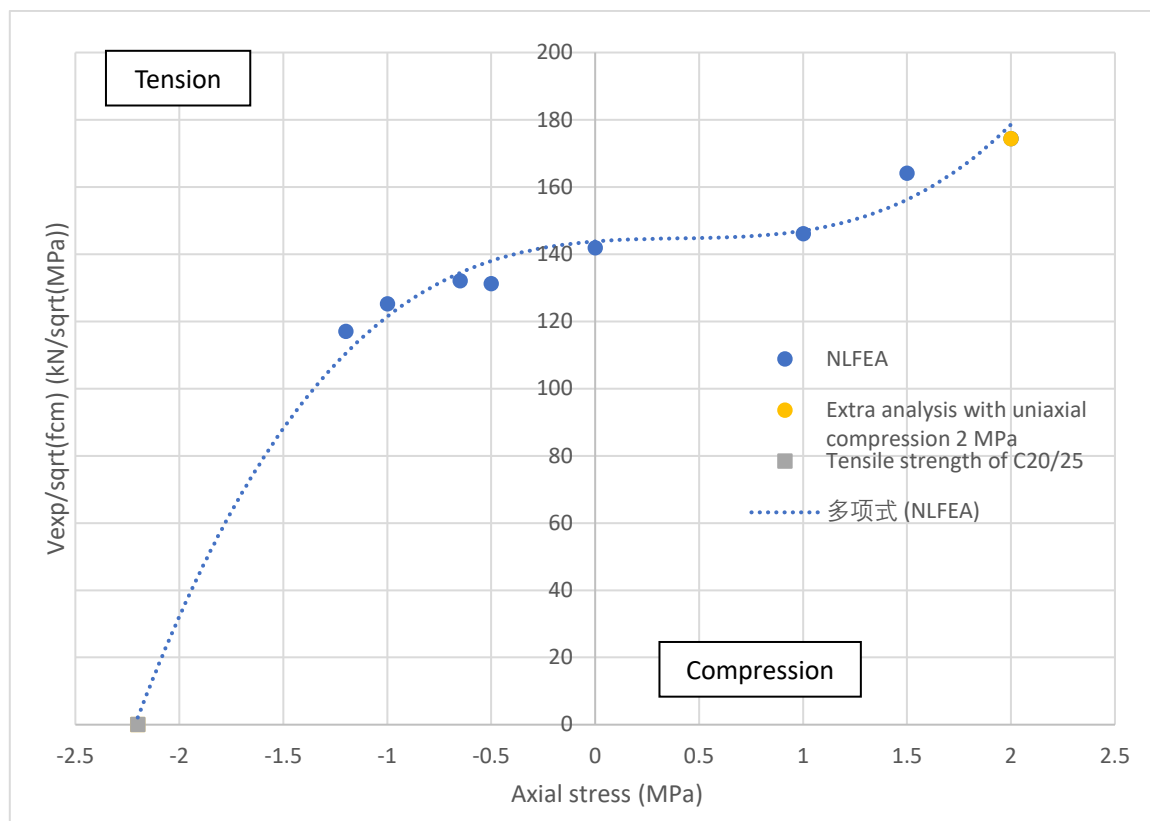


Figure 46 Influence of uniaxial load on shear capacity of modelling

In terms of the influence of uniaxial compression, the shear load – displacement figures of S2, SC1 and SC2 are selected and compared. From this figure, it can be concluded that axial compression improves the shear capacity. Higher compression, higher increase. What's more, axial compression improves the stiffness of slab after cracking. And initial flexural crack force is delayed by axial compression (194 kN in SC1 while 131 kN in S2). Uniaxial compression increases the elastic stiffness as well. The stiffness of SC1 and SC2 does not differ apparently. The same situation is demonstrated by Bui *et al.* (2017). However, it is stated in Bui *et al.* (2017) that the more axial compression is applied, the more the elastic stiffness is increased. Although uniaxial compression increases the shear capacity of slab, it also leads to brittle behaviour after peak load.

When it comes to the uniaxial tension, shear capacity of the slab is decreased when it is loaded in uniaxial tension. Higher tension, lower shear capacity. In addition, axial tension decreases the elastic stiffness of slab. Initial flexural crack force is reached early when loaded in axial tension (125 kN in SC3 while 131 kN in S2). When the ultimate load was reached, the specimens demonstrated a softening response, with a large reduction in the applied force for increasing deflections. These results are stated in Bui *et al.* (2018) as well. Figure 47 shows the modelling results of slabs under compression and tension respectively. It is stated in experiment that the higher the axial tension, the steeper the diagonal compression inclination

from the loading area. However, this phenomenon is not found in NLFEA. This is caused by using fixed crack model in concrete material. When applying rotating crack model, the inclination changes.

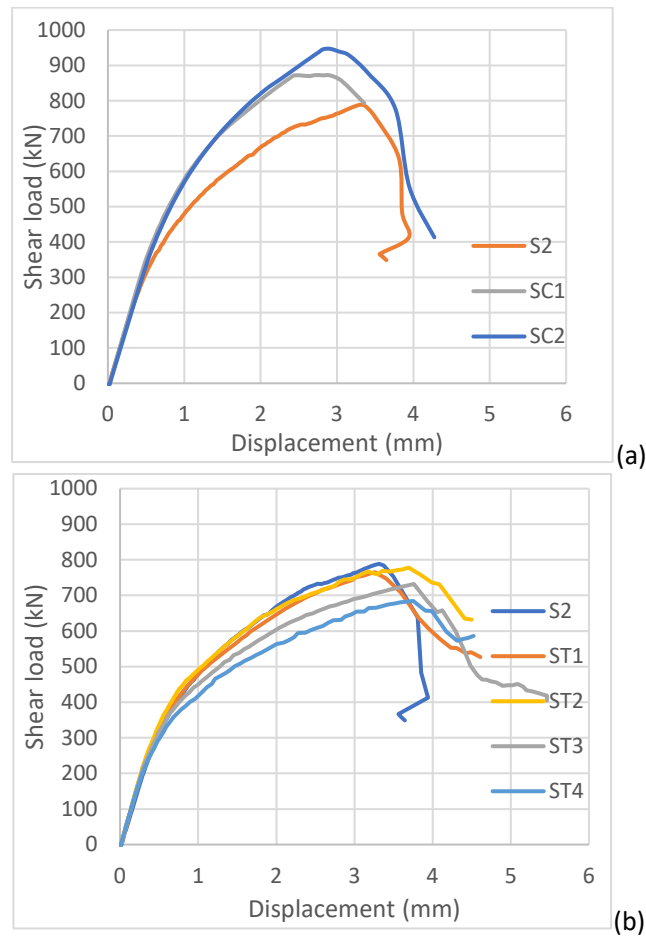


Figure 47 Influence of uniaxial loads on shear capacity: a) Compression; b) Tension

4.4 Discussion of results

4.4.1 Influence of uniaxial load on the shear capacity

It can be concluded according to chapter 4 that the NLFEA in this master thesis shows that the influence of uniaxial in-plane load on the shear capacity of single slabs is valid when compared to the results from experiment. However, some difference exists. The Figure 48 shows the comparison.

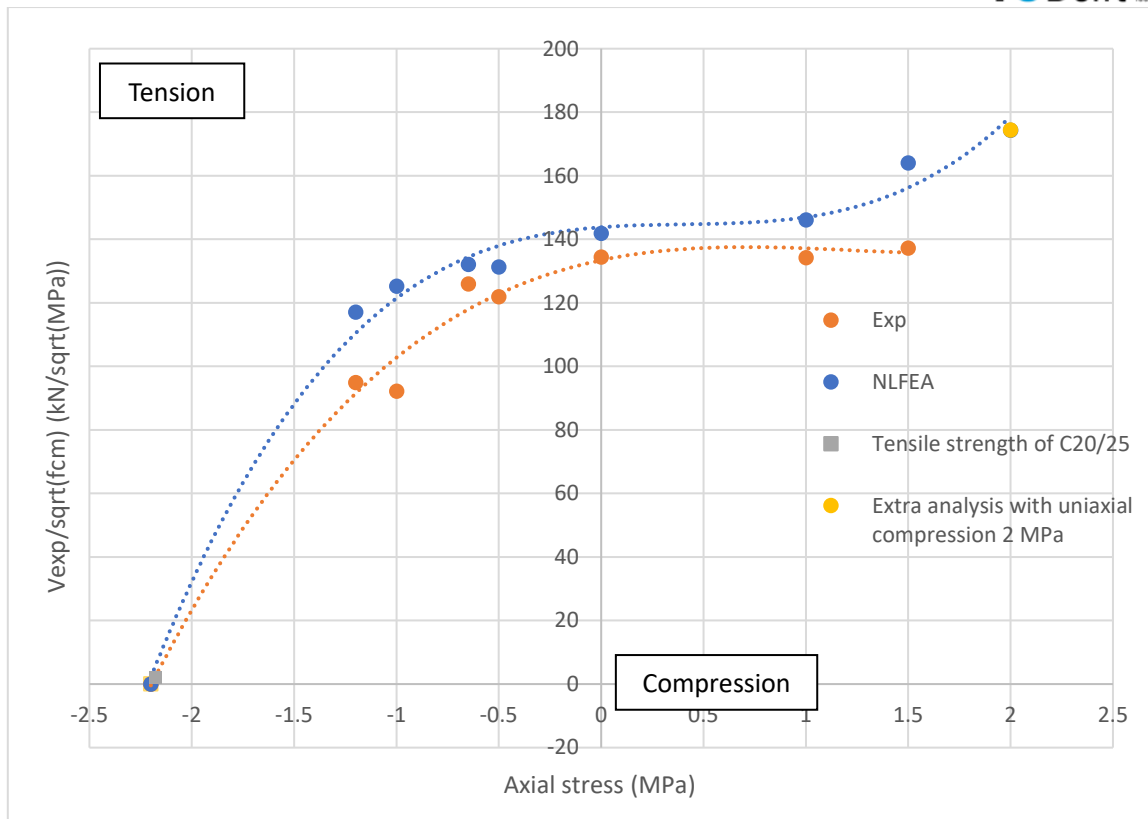


Figure 48 Comparison of influence of uniaxial load between NLFEA and experiment

The same phenomenon is observed in both experiment and NLFEA that uniaxial compression delays the initial flexural crack and tension decrease the force when the initial crack occurs. When loaded in uniaxial tension, the initial crack occurs at 106 kN in ST4 and 131 kN in S2 in NLFEA, while 15 kN in ST4 and 125 kN in S2 in experiment. When it comes to uniaxial compression, the initial crack occurs at 194 kN in SC1 and 131 kN in S2 in NLFEA, while 190 kN in SC1 and 125 kN in S2 in experiment.

In experiment, it is stated that uniaxial in-plane tension values equal to $0.28f_{ctm}$ of the concrete tensile resistance reduce the shear capacity up to 30. In NLFEA, the influence of incremental uniaxial tension on the shear capacity is smaller than experiment which is indicated by ST3 that $0.28f_{ctm}$ reduces the shear capacity about 8%. And incremental uniaxial compression in NLFEA has larger influence. In experiment it is stated that the influence of uniaxial compression is not obvious because of the relatively small value of compressive load compared to the concrete compressive strength. However, NLFEA shows a larger influence when the same compressive load is applied which is indicated by SC2, that is, 1.5 MPa of uniaxial in-plane compression increase the shear capacity by 6% in experiment but 20% in NLFEA. Uncertainties exist in experiment and the conclusion in this aspect is not easy to be drawn with only seven samples. More researches including experiments and numerical analysis are needed to better investigate the influence of uniaxial load on shear capacity of RC slabs without shear reinforcement.

4.4.2 Validation of nonlinear finite element analysis on RC slab loaded in uniaxial force

Based on the research results from Bui *et al.* (2017), the comparison of prediction of shear capacity from EC2, ACI 318-14, experiment and NLFEA is made. By analyzing the prediction of shear capacity, the validation of nonlinear finite element analysis on RC slab loaded in uniaxial force can be found. Figure 49 and Table 17 show the comparison among shear capacity of each slab, from experiment, analytical assessment and the NLFEA results in this thesis. The calculation of shear capacity from EC2 and ACI 318-14 can be found in Annex, which is indicated in chapter 2.1 as well. Results of analytical calculation are listed in Table 116. Note that the calculation in EC2 is the formula for one-way shear. In addition, based on the data in this figure, the calculation of variance is made to analyze the validation of each method.

Table 16 Shear strength prediction

Slab	Axial stress σ_{cp} [Mpa]	$f_{cm,cyl}$ [Mpa]	V_{exp} [kN]	V_{EC2} [kN]	$V_{ACI\ 318-14}$ [kN]	V_{NLFEA} [kN]
SC2	1.5	33.3	792	581	473	947
SC1	1.0	35.6	801	539	458	872
S2	0.0	30.9	747	455	427	788
ST1	-0.5	34.0	711	412	366	765
ST2	-0.65	34.7	742	400	348	778
ST3	-1.0	34.2	539	370	305	732
ST4	-1.2	34.2	555	253	281	684

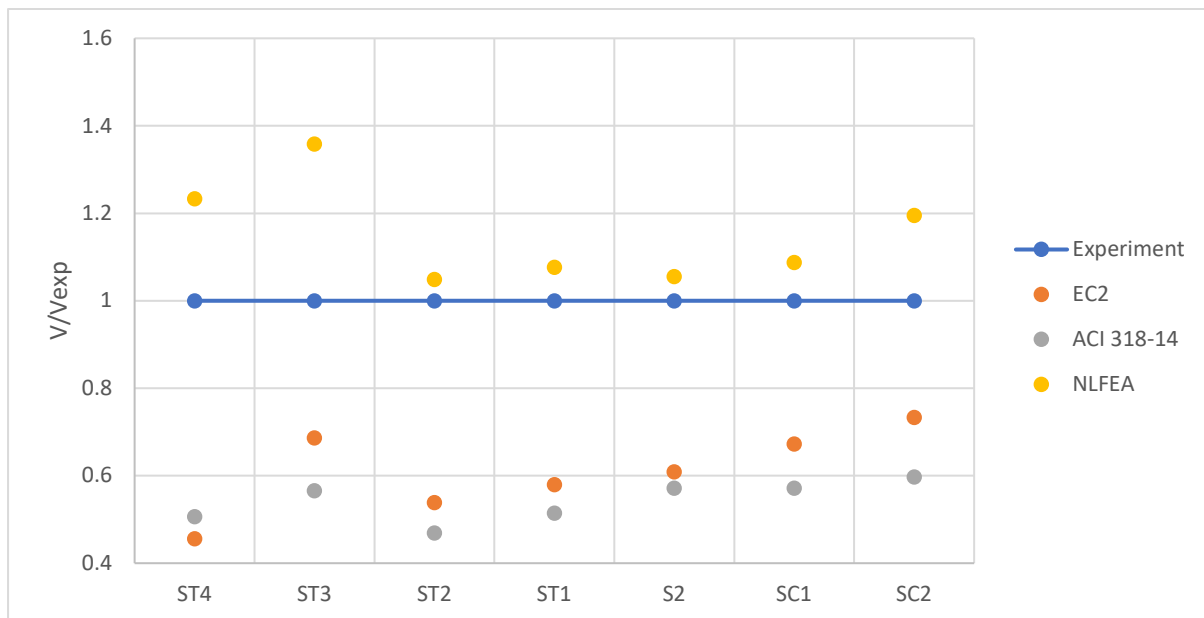


Figure 49 Comparison of predictions from various methods

Table 17 Results of predictions from various methods

	ST4	ST3	ST2	ST1	S2	SC1	SC2	Average	Variance
Exp	1	1	1	1	1	1	1	1	0
EC2	0.46	0.69	0.54	0.58	0.61	0.67	0.73	0.61	0.01
ACI 318-14	0.51	0.57	0.47	0.51	0.57	0.57	0.60	0.54	0.00
NLFEA	1.23	1.36	1.05	1.08	1.06	1.09	1.20	1.15	0.01

Firstly, the prediction of shear capacity of RC slabs without shear reinforcement from NLFEA is larger than experiment for each slab. NLFEA produces overestimated results, while EC2 and ACI 318-14 are relatively conservative. Prediction of analytical assessment coincides with the theory that larger uniaxial in-plane tension leads to lower shear capacity and larger in-plane compression leads to higher shear capacity. Experiment contains the uncertainty. Note that the inputs used in analytical assessment and NLFEA are the values from tests in experiment, that is to say, the safety factor is all assumed to be 1. Due to the unconservative prediction of NLFEA, it is interesting to apply safety formats on NLFEA for security cases. NLFEA with safety formats, which is introduced in Dutch Guideline (Hendriks *et al.*, 2017) and MC 2010, is suggested in further study to dealing with the uncertainties.

5. Conclusion

The objective of this master thesis is to investigate the validation of nonlinear finite element analysis on the RC slabs without shear reinforcement under uniaxial loads. After the study about previous literature, the investigation of cases from Bui *et al.* (2017) and Nana *et al.* (2017), the simulation of case study by NLFEA, comparison and discussion about the results, conclusion can be made and summarized in two sections about slabs without uniaxial in-plane load and with uniaxial in-plane loads respectively. Suggestions for further study are made as well.

5.1 Conclusion of slab without uniaxial in-plane load

Conclusion of slab without uniaxial in-plane load can be summarized as below:

- When it comes to the shear load – displacement curve, nonlinear finite element shows the similar stiffness as experiment when cracks do not occur. However, stiffer behaviour is observed in NLFEA during the development of cracks. This is similar to the NLFEA results from Nana *et al.* (2017).
- It is suggested by Nana *et al.* (2017) that the reason for the stiffness difference is the lack of mortar layer. However, the alternative NLFEA by modelling the mortar layer with interface in this thesis shows that lack of mortar layer is not the reason for stiffness difference.
- Alternative NLFEA proves that fracture energy, rotating crack are not the main reason for the stiffer structural behaviour in NFLEA.
- Although the results of alternative NLFEA with bond-slip reinforcement show the stiffer structural behaviour still, it cannot prove that bond-slip reinforcement is not the main reason for stiffness differenc. This is because that the few attempts are not sufficient enough to make the conclusion that whether bond-slip reinforcement is the reason for stiffer structural behaviour.
- Development of crack pattern observed in NLFEA is similar to the experiment. In experiment, the development of punching shear cone is observed but the failure mode is described as one-way shear that the crack near the edge of steel support is the indication. However, the crack pattern in NLFEA of this thesis is similar to Nana *et al.* (2017) that the crack near the steel support is not observed. The diagonal crack from the edge of loading plate developed, of which the crack width increases with increment of loading and finally cause the failure of structure at the peak load stage (with crack width 2.27 mm for S2 in NLFEA of this thesis). This indicates that the failure mode of slabs in NLFEA is due to punching.

5.2 Conclusion of slabs with uniaxial in-plane load

Conclusion of slabs with uniaxial in-plane load can be summarized as below:

- It is stated in experiment that uniaxial tension decreases the elastic stiffness while compression increases it. The larger tensile force is applied, the more reduction is. The reduction of stiffness when the slab is loaded in in-plane tension is proved in NLFEA. Nevertheless, the increase of elastic stiffness in NLFEA is not obvious due to the relatively small value of uniaxial compressive stress (1 MPa for SC1 and 1.5 MPa

for SC2) compared with concrete compressive strength (35.6 MPa for SC1 and 33.3 MPa for SC2).

- Experiment shows that uniaxial tension reduces the shear capacity of structure while compression increases it. The more uniaxial tension (compression) is applied, the more reduction (increase) of shear capacity is. The same tendency is observed in NLFEA. However, as the discussion in chapter 4.4, this influence of increasing uniaxial compression in NLFEA is larger than that in experiment, while less influence on shear capacity with increasing uniaxial tension. Due to the small number of experimental samples, the reason for this phenomenon is not easy to draw.
- In experiment, uniaxial tension leads to ductile structural behaviour while compression leads to brittle structural behaviour in post peak load phase. This coincides with the results from NLFEA.
- The experiment and NLFEA both prove that uniaxial compression increases the initial flexural cracking force and the tension decreases it, which means that the uniaxial compression delays the initial flexural cracking as is discussed in chapter 4.4.
- In experiment, the diagonal compression inclination from the loading area to the edge of steel support changes due to uniaxial in-plane load. The larger the tension, the steeper this inclination is. However, this phenomenon is not observed in the NLFEA. Using fixed crack concrete model in modelling could lead to this because the direction of cracks cannot change once they are initiated. Changing fixed crack concrete model to rotating crack model can solve this problem.

When it comes to the prediction of shear capacity for all slabs, nonlinear finite element analysis gives overestimated results. On average, shear capacity is overestimated 15% more than the results from experiment. While EC2 and ACI 318-14 produce conservative results by 8% lower than experiment of EC2 and 30% lower of ACI 318-14 on average.

5.3 Suggestions for further study

Suggestions for further study can be summarized below:

- In aspect of the interpretation of stiffer structural behaviour in NLFEA, using finer mesh in modelling is suggested. Finer mesh can result in more accurate structural behaviour, such as crack pattern, shear capacity and stiffness.
- Improvement and insights of NLFEA with bond-slip reinforcement is suggested to verify whether the bond-slip reinforcement is the reason for the stiffer structural behaviour in NLEFA.
- The uncertainty due to random variation of material properties exists in the experiment. Taking the material inputs from experiment introduces this uncertainty into modelling. Performing the NLEFA with safety formats following MC 2010 and Dutch Guideline (Hendriks *et al.*, 2017) is suggested in further study to reduce the influence of this uncertainty. Then, the safer predictions of shear capacity from NLFEA can be expected as well.
- The difference between experiment and NLFEA occurs that the influence from the increasing uniaxial in-plane force on the shear capacity of slabs in NLFEA is different from that in experiment. More experiments are needed, about RC slabs loaded in

concentrated out-of-plane load and uniaxial in-plane load, to verify the influence of increasing uniaxial in-plane compression on shear capacity of slabs. Then, NLFEA on RC slabs can be validated more clearly by applications on experiments.

Reference

- Belletti, B., Damoni, C., Hendriks, M., & Boer, A. de. (2014). Analytical and numerical evaluation of the design shear resistance of reinforced concrete slabs. *Structural Concrete*, 317–330.
- Bui, T., Abouri, S., Limam, A., Nana, W., Tedoldi, B. and Roure, T. (2017). Experimental investigation of shear strength of full-scale concrete slabs subjected to concentrated loads in nuclear buildings. *Engineering Structures*, 131, pp.405-420.
- Bui, T., Nana, W., Abouri, S., Limam, A., Tedoldi, B. and Roure, T. (2017). Influence of uniaxial tension and compression on shear strength of concrete slabs without shear reinforcement under concentrated loads. *Construction and Building Materials*, 146, pp.86-101.
- Building code requirements for structural concrete (ACI 318-14). (2014). Farmington Hills: American Concrete Institute.
- CEN (2004a) EN 1992-1-1: Eurocode 2: Design of concrete structures – Part 1-1: General rules and rules for buildings.
- CEN (European Committee for Standardization) (2002a) EN 1990: Eurocode – Basis of structural design.
- DIANA – Finite Element Analysis, User’s Manual Release 10.1. Material Library – Background, DIANA FEA BV, 2010, pp. pages 405-406.
- Engen, M. (2017). Aspects of design of reinforced concrete structures using non-linear finite element analyses: Solution strategy, modelling uncertainty and material uncertainty.
- fib. (2013). Model Code for Concrete Structures 2010. Lausanne: International Federation for Structural Concrete (fib).
- Hendriks, M. A. N., den Uijl, J. A., de Boer, A., Feenstr, P. H., Belletti, B., & Damoni, C. (2017). Guidelines for nonlinear finite element analysis of concrete structures. (ver. 2.1). Delft: Rijkswaterstaat Centre for Infrastructure.
- Hopkins, D. C. (1969). Effects of membrane action on the ultimate strength of reinforced concrete slabs. University of Canterbury. Department of Civil Engineering.
- Lantsoght, E. O. L. (2013). Shear in Reinforced Concrete Slabs under Concentrated Loads Close to Supports. Tesis Doctoral.
- Lantsoght, E., Veen, C., & Walraven, J. (2014). Shear in One-Way Slabs under Concentrated Load Close to Support. *ACI Structural Journal*, (110), 275–284.
- Lantsoght, Eva & Veen, Cor & Hordijk, Dick & Boer, Ane. (2017). Recommendations for proof load testing of reinforced concrete slab bridges.

- Limam, S., Nana, W., Bui, T., Limam, A. and Abouri, S. (2017). Experimental investigation and analytical calculations on shear strength of full-scale RC slabs with shear reinforcement for nuclear power plants. *Nuclear Engineering and Design*, 324, pp.143-157.
- Nana, W., Bui, T., Limam, A. and Abouri, S. (2017). Experimental and Numerical Modelling of Shear Behaviour of Full-scale RC Slabs Under Concentrated Loads. *Structures*, 10, pp.96-116.
- Regan, P. E. (1982). *Shear Resistance of Concrete Slabs at Concentrated Loads close to Supports*. London, United Kingdom.
- Regan, P. E. (1987). *Shear Resistance of Members Without Shear Reinforcement proposal for CEB Model Code MC90*. CEB COMMISSION IV, TREVISO, MAY 1987.
- Regan, P. E., & Rezai-Jorabi. (1988). Shear Resistance of One-Way Slabs Under Concentrated Loads. *Structural Journal*, 85(2).
- Schlune, H., Plos, M., Gylltoft, K.: *Safety Formats for Non-linear Analysis of Concrete Structures*. *Engineering Structures*, Elsevier, vol. 33, No. 8, Aug 2011.
- Shu, J. (2017). *Structural analysis methods for the assessment of reinforced concrete slabs*. Chalmers University of Technology.
- Timoshenko, S., Woinowsky-Krieger, S., (1959). *Theory of Plates and Shells*. McGrawHill.

Annex – calculation of shear capacity according to EC2 and ACI 318-14

1. Eurocode 2

In Eurocode 2, the calculation of shear strength for members not requiring design shear reinforcement is shown in chapter 2.1. That is:

$$V_{Rd,c} = \left[C_{Rd,c} k (100 \rho_l f_{ck})^{1/3} + k_1 \sigma_{cp} \right] b_w d$$

With the minimum of:

$$V_{Rd,c} = (v_{\min} + k_1 \sigma_{cp}) b_w d$$

And the minimum shear stress is:

$$v_{\min} = 0.035 k^{3/2} \cdot f_{ck}^{1/2}$$

Using concrete of C20/25, the characteristic compressive strength is $f_{ck} = 20 \text{ MPa}$,

The assumption is made that the effective width of shear load distribution is 45° from the far end of loading plate. The b_w is calculated according to this assumption.

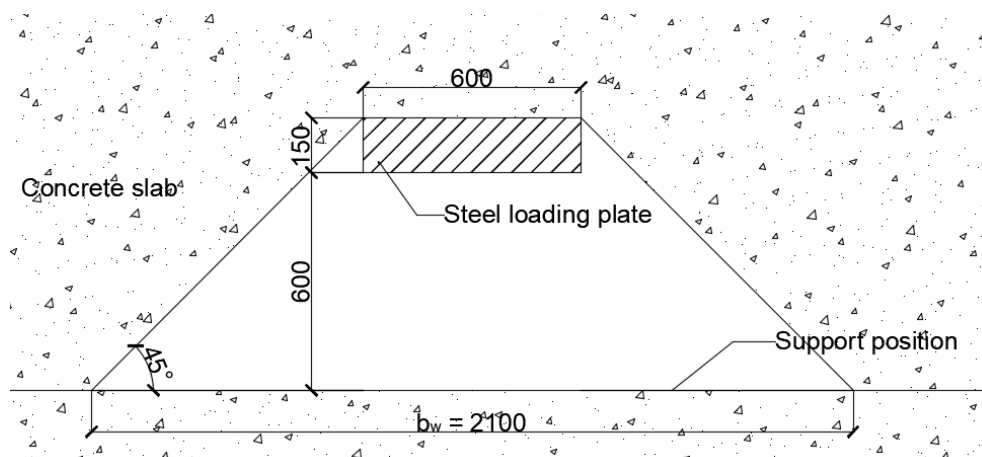


Figure A Effective width of shear load distribution

Effective depth of the cross section d is defined from the top of concrete to the middle of bottom layer of reinforcement.

Reinforcement ratio is the longitudinal reinforcement ratio in experiment.

The value of k is determined as $k = 1 + \sqrt{\frac{200}{d}} = 1.86 < 2$.

The value of k_1 is advised as 0.15.

It is assumed that material partial factor is $\gamma_c = 1$.

$C_{Rd,c}$ is the factor derived from tests. The recommended value in Eurocode 2 is $0.18 / \gamma_c$. In

this calculation, this factor is to determine the average value of experiments. The value is cited as $C_{Rd,average} = 0.15$ according to Regan (1987).

The parameters for each slab are summarized in Table A:

Table A Parameters for calculation

Slab	Axial stress σ_{cp} [Mpa]	f_{ck} [Mpa]	b_w [mm]	d [mm]	ρ_l [%]	$C_{Rd,average}$	k	k_1
SC2	1.5	20	2100	267.5	1.223	0.15	1.86	0.15
SC1	1.0	20	2100	267.5	1.223	0.15	1.86	0.15
S2	0.0	20	2100	267.5	1.223	0.15	1.86	0.15
ST1	-0.5	20	2100	267.5	1.223	0.15	1.86	0.15
ST2	-0.65	20	2100	267.5	1.223	0.15	1.86	0.15
ST3	-1.0	20	2100	267.5	1.223	0.15	1.86	0.15
ST4	-1.2	20	2100	267.5	1.223	0.15	1.86	0.15

Note that in the calculation, uniaxial in-plane compression is positive and tension is negative.

The results of all slabs are:

Table B Shear capacity prediction of EC2

Slab	SC2	SC1	S2	ST1	ST2	ST3	ST4
Axial stress σ_{cp} [Mpa]	1.5	1.0	0.0	-0.5	-0.65	-1.0	-1.2
V_{EC2} [kN]	581	539	455	412	400	370	253

2. ACI 318-14

The simplified method of calculation of shear capacity is used. The formula for members loaded in tension and compression are slightly different.

For tension:

$$V_c = 0.17 \left(1 + \frac{N_u}{3.5A_g} \right) \lambda \sqrt{f'_c} b_w d$$

For compression:

$$V_c = 0.17 \left(1 - \frac{N_u}{14A_g} \right) \lambda \sqrt{f'_c} b_w d$$

The unit used here is metric.

f'_c is the specified compressive strength of concrete, which is 20 MPa in this case.

A_g is the gross area of concrete section, which is:

$$A_g = b_w \cdot d = 561750 \text{mm}^2$$

N_u is the axial load, which is calculated as:

$$N_u = \sigma_{cp} \cdot b_w \cdot d$$

Note that uniaxial compression is positive and tension is negative.

Thus, the prediction of shear capacity from ACI 318-14 is summarized below:

Table C Shear capacity prediction of ACI 318-14

Slab	SC2	SC1	S2	ST1	ST2	ST3	ST4
Axial stress σ_{cp} [Mpa]	1.5	1.0	0.0	-0.5	-0.65	-1.0	-1.2
V _{ACI 318-14} [kN]	473	458	427	366	348	305	281